AD-A041 717 SOLAR SAN DIEGO CALIF F/G 21/5
DESIGN AND DEVELOPMENT OF A MAJOR ENGINE COMPONENT (COMPRESSOR)--ETC(U)
JUN 77 R GODDARD, D J MARTIN DAAK02-73-C-0398
UNCLASSIFIED ER-2561 NL

1 OF 1
ADA041717

END
DATE
FILMED
8 - 77

AD A041717

AD

ER 2563

DESIGN AND DEVELOPMENT OF A MAJOR ENGINE COMPONENT (COMPRESSOR) FOR A 60-KW TURBINE GENERATOR SET

FINAL REPORT

by

Robert [illegible]

&

Douglas J. Martin

JUNE 1977

for

US ARMY MOBILITY EQUIPMENT RESEARCH AND
DEVELOPMENT COMMAND
ELECTRICAL POWER LABORATORY
Ft. BELVOIR, Va. 22060
Prepared Under Contract No. DAAK02-73-C-0398

by

Solar, an International Harvester Company Group
2200 Pacific Highway
San Diego, California 92112

DISTRIBUTION OF THIS REPORT IS UNLIMITED

AD

ER 2563

DESIGN AND DEVELOPMENT
OF A MAJOR ENGINE COMPONENT (COMPRESSOR)
FOR A 60-KW TURBINE GENERATOR SET

FINAL REPORT

by

Robert Goddard

&

Douglas J. Martin

JUNE 1977

for

U.S. ARMY MOBILITY EQUIPMENT RESEARCH AND
DEVELOPMENT COMMAND
ELECTRICAL POWER LABORATORY
FT. BELVOIR, VA 22060
Prepared Under Contract No. DAAK02-73-C-[illegible]

by

Solar, an International Harvester Company Group
2200 Pacific Highway
San Diego, California 92112

DISTRIBUTION OF THIS REPORT IS UNLIMITED

Disclaimer

The findings in this report are not to be construed as an official Department of the Army position, unless so designated by other authorized documents.

The citation of trade names and names of manufacturers in this report is not to be construed as official Government endorsement or approval of commercial products or services referenced herein.

Disposition Instructions

Destroy this report when it is no longer needed. Do not return it to the originator.

Unclassified

Security Classification

DOCUMENT CONTROL DATA - R & D

[illegible]

Solar Turbines International, an International Harvester Group, San Diego, California [illegible]

Unclassified

N/A

Design and Development of a Major Engine Component (Compressor) for a 10 kW Turbine Generator Set

Final Technical, Design and Development

Final rept.

Robert [illegible] Goddard

Douglas [illegible] Martin

[illegible]

Distribution of This Report is Unlimited

U.S. Army Mobility Equipment Research and Development Command, Electrical Power Laboratory, Ft. Belvoir, VA

This report documents the design and development of an advanced gas turbine compressor [illegible] 10 kW [illegible] generator set. [illegible]

[illegible]

DD FORM 1473

Unclassified

Security Classification

[illegible]

Unclassified

Security Classification

KEY WORDS	LINK A		LINK B		LINK C	
	ROLE	WT	ROLE	WT	ROLE	WT
Compressors, Centrifugal, Gas Turbine Generator Set						

Unclassified

Security Classification

SUMMARY

[illegible]

[illegible]

[illegible]

[illegible]

[illegible]

[illegible]

[illegible]

[illegible]

FOREWORD

The developmental work documented in this report was carried out under Contract No. [illegible], awarded by the U.S. Army Mobility Equipment Research and Development Command, Fort Belvoir, Virginia 22060.

The technical representative of the U.S. Army was Mr. [illegible]. The principal investigators responsible for the technical content, execution, and success of the program were [illegible] and [illegible].

TABLE OF CONTENTS

Section		Page
	SUMMARY	iii
1	INTRODUCTION	1
	1.1 BACKGROUND	1
	1.2 PERFORMANCE OBJECTIVES	2
2	DESIGN APPROACH	3
	2.1 GENERAL	3
	2.2 ENGINE RIG CONFIGURATION	3
	2.2.1 Compressor Design Details	5
	2.2.2 Turbine Design Details	8
	2.2.3 Critical Speed Analysis	[illegible]
	2.2.4 Rotor Bearing and Lube System Design	[illegible]
	2.2.5 Rotor Assembly	[illegible]
	2.2.6 Seal Plate Assembly	[illegible]
	2.2.7 Air Side Housing	[illegible]
	2.2.8 Diffuser	22
	2.2.9 Turbine Scroll	22
	2.2.10 Combustor Assembly	22
	2.2.11 Fuel System	22
3	ENGINE TEST RIG	[illegible]
	3.1 DESCRIPTION OF INSTALLATION	[illegible]
	3.2 INSTRUMENTATION	[illegible]
4	DEVELOPMENT PROGRAM	[illegible]
	4.1 INITIAL BALANCE PROCEDURES	[illegible]
	4.2 BLADE RESONANCE TESTS	[illegible]
	4.3 ENGINE RIG ASSEMBLY	[illegible]
	4.4 ROTOR EXCURSION MEASUREMENTS	[illegible]
	4.5 RIG OPERATIONAL TESTS	[illegible]
	4.6 ROTOR THRUST MEASUREMENTS	[illegible]

TABLE OF CONTENTS (Cont)

Section		Page
5	DISCUSSION	53
	5.1 ROTOR BALANCE	54
	5.2 TURBINE NOZZLE SHIFT	54
	5.3 BEARING/SHAFT PROBLEMS	54
6	PERFORMANCE	57
	6.1 ESTIMATED PERFORMANCE	57
	6.2 TEST PERFORMANCE	59
	6.2.1 Compressor Performance	60
	6.2.2 Turbine Performance	65
	6.2.3 Engine Performance	71
7	PRELIMINARY ENGINE DESIGN AND PACKAGING	75
8	CONCLUSION	78

LIST OF ILLUSTRATIONS

Figure		Page
1	Advanced 60-kW Engine Test Rig	4
2	Engine Test Rig (Turbine Power Section)	6
3	Component Test Rig	7
4	Engine Compressor	8
5	Rig Test Compressor Performance	10
6	Engine Radial Inflow Turbine	11
7	Turbine Rig Performance	12
8	Engine Critical Speeds	14
9	Instrumented Rotor Bearing Capsules	15
10	Turbine Rotor, Bearing Capsule, and Pinion Assembly	16
11	Engine Estimated End Thrust	17
12	Rotor Assembly Showing Curvic Coupling in Mesh	19
13	Compressor Curvic Coupling	20
14	Engine Rig Seal Plate	21
15	Air Inlet Housing and Rotor Adapter Retaining Plate	23
16	Air Inlet Housing and Compressor Diffuser	24
17	Air Inlet Housing with Turbine Assembly Installed (Front View)	25
18	Turbine Nozzle Assembly	26
19	Combustor Housing	27
20	Engine Rig Test Cell Schematic	31
21	Aft View of Engine Test Rig Installed in Test Cell	32
22	Power Turbine Section Pressure/Temperature Instrumentation	33
23	Turbine Nozzle Pressure/Temperature Instrumentation	34
24	Air Inlet Assembly Instrumentation	35
25	Combustor Assembly Instrumentation	36
26	Turbine Nozzle Instrumentation	37

LIST OF ILLUSTRATIONS (Cont)

Figure		Page
27	Engine Build Clearance Chart	43
28	Rotor Proximity Probes and Positioning Fixture	45
29	Spectral Analyzer Track of Rig Cranking Test	46
30	Conventional Nozzle Pinning Modification	48
31	Bearing Thrust Monitoring Device	50
32	Proposed Design Changes for the Prototype Engine	55
33	Engine Estimated Performance	58
34	Effect of Inlet Temperature	59
35	Compressor Performance (0.020-Inch Shroud Clearance)	61
36	Compressor Performance (0.014-Inch Shroud Clearance)	63
37	Compressor Performance (With Additional Spring Seal)	64
38	Effect of Shroud Curvature	65
39	Impeller Modification	66
40	Final Compressor Calibration	67
41	Turbine Performance (First Calibration)	68
42	Turbine Performance (Second Calibration)	69
43	Turbine Performance (Scalloped Configuration)	70
44	Engine Performance (Final Calibration)	72
45	Engine Performance Test Data	73
46	Advanced Turbine Test Performance Data	74
47	Advanced Engine Cross Section	76

LIST OF TABLES

Table		Page
1	Compressor Major Aerodynamic Performance Parameters	9
2	Turbine Major Aerodynamic Performance Parameters	13
3	Aerodynamic Performance and Mechanical Test Instrumentation	38
4	Engine Cycle Conditions, Installed in EMU-30/E Generator Set	60

1

INTRODUCTION

1.1 BACKGROUND

Contract DAAK02-73-C-0398 was awarded by the U.S. Army Mobility Equipment Research and Development Center to Solar Division of International Harvester in June of 1973. This contract was awarded as a result of a Request for Quote, DAAK02-73-Q-0099, which called for development proposals for a "state of the art" gas turbine engine compressor to be used on a new 60-kW gas-turbine-powered generator set.

Specifically, the contract called for the design of a compressor, its incorporation into a test rig, and tests to confirm the aerodynamic performance of the design. In addition, a conceptual design was to be prepared for an engine to meet the requirements of the U.S.A. MERDC Purchase Description "Generator Set, Gas Turbine Driven, Alternating Current, 60-kW", and a basic plan was required for utilization of the new engine in a generator set.

Solar had already completed the design and component rig test of an advanced compressor and turbine, both of which met the precise requirements specified in the quotation request. Solar therefore proposed a program to install these components in a simulated engine test rig as the next logical step in the development process.

This proposed engine test rig would be used to confirm the design parameters established on the individual component rigs and to provide a basic configuration for the new prototype engine.

In addition, since Solar was in production with a 60-kW generator set to the required Purchase Description (the EMU-30/E), the prototype engine was designed as a direct physical replacement for the existing generator set Titan T-62T-32 gas turbine engine. New primary reduction gearing would be required to reduce the new high-performance engine speed to the required output, but almost all of the existing package components would be retained. Thus, the prototype would represent not only an engine for future applications but also a retrofit unit to improve the fuel consumption and reliability of the existing approximately one thousand generator sets in the military inventory.

The U.S. Army Mobility Equipment Research and Development Center accepted the Solar recommendation, and work on the program proceeded on that basis.

1.2 PERFORMANCE OBJECTIVES

The performance improvements expected as the result of this contract were defined in the contractual documents only in the following general terms. The compressor was envisioned as being a key item in the new engine, which would be required to meet a 72 lb/hour maximum fuel flow at 10-kW output with an alternator of 0.88 efficiency.

Inlet and exhaust pressure losses for the new generator set were specified as 2 percent and 3 percent respectively, and the inlet temperature for the installed engine was specified as 10°F higher than the 60°F ambient, sea level conditions. "Worst case" ambient conditions were identified as 5000-foot altitude with an ambient temperature of 107°F.

As a guideline, the specification envisioned a compressor pressure ratio of between 5 and 6 to 1, with a total static adiabatic efficiency approaching 0.80.

This report will show that the component test rig work already accomplished and the overall performance measured on the engine test rig demonstrate compliance with the operational requirements and agree with the compressor performance projections contained in the specification.

Specific details of the test performance achieved are presented in some detail in Section 6, Performance.

2

DESIGN APPROACH

2.1 GENERAL

2.2 ENGINE TEST RIG CONFIGURATION

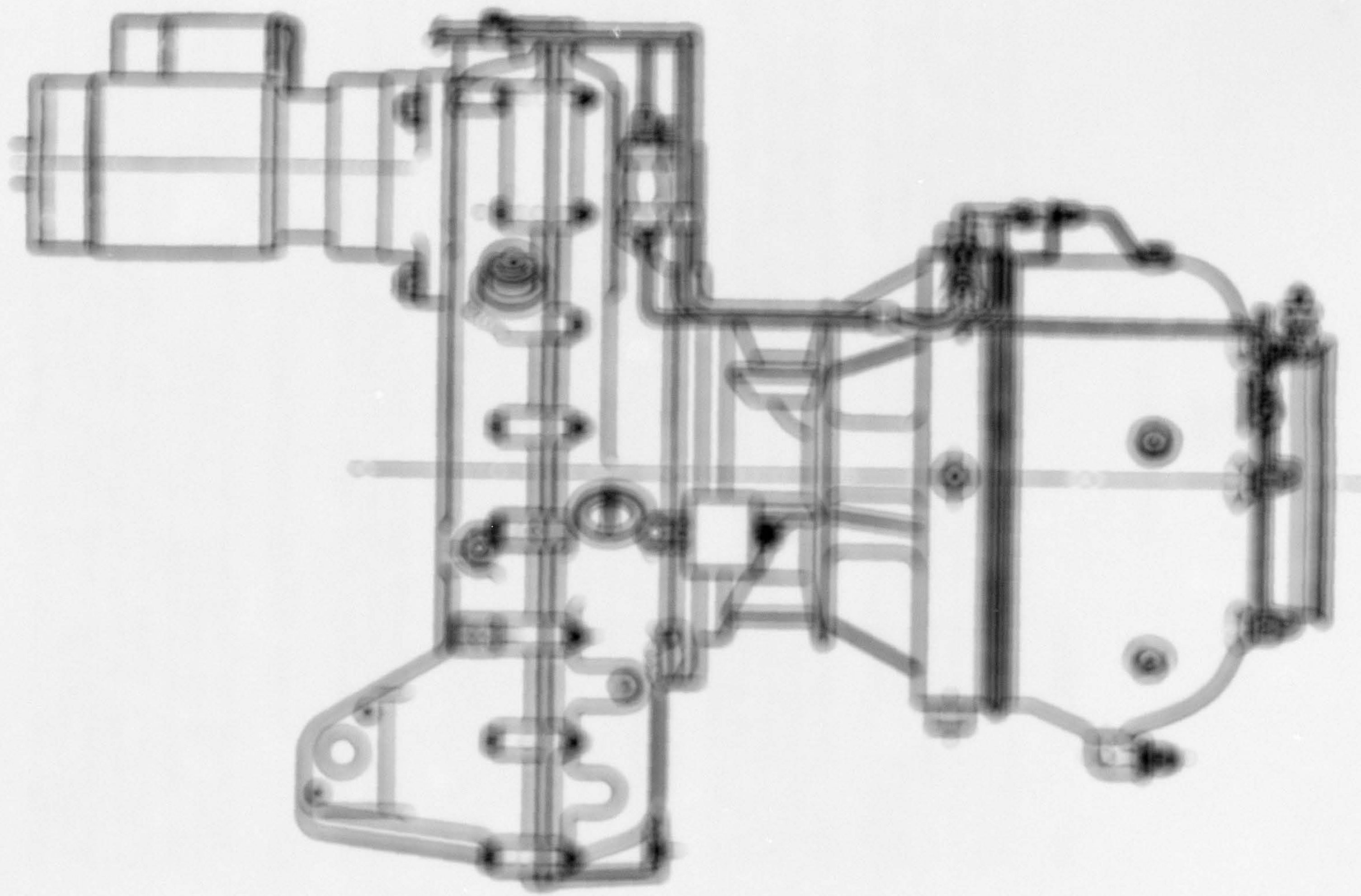

Figure [illegible]. Advanced [illegible] Engine Test Rig

[illegible]

Specific details of the design of the individual components are as follows:

[illegible] Compressor Design Details. [illegible]

[illegible]

[illegible]

[illegible] Turbine Design Details. [illegible]

[illegible]

[illegible]

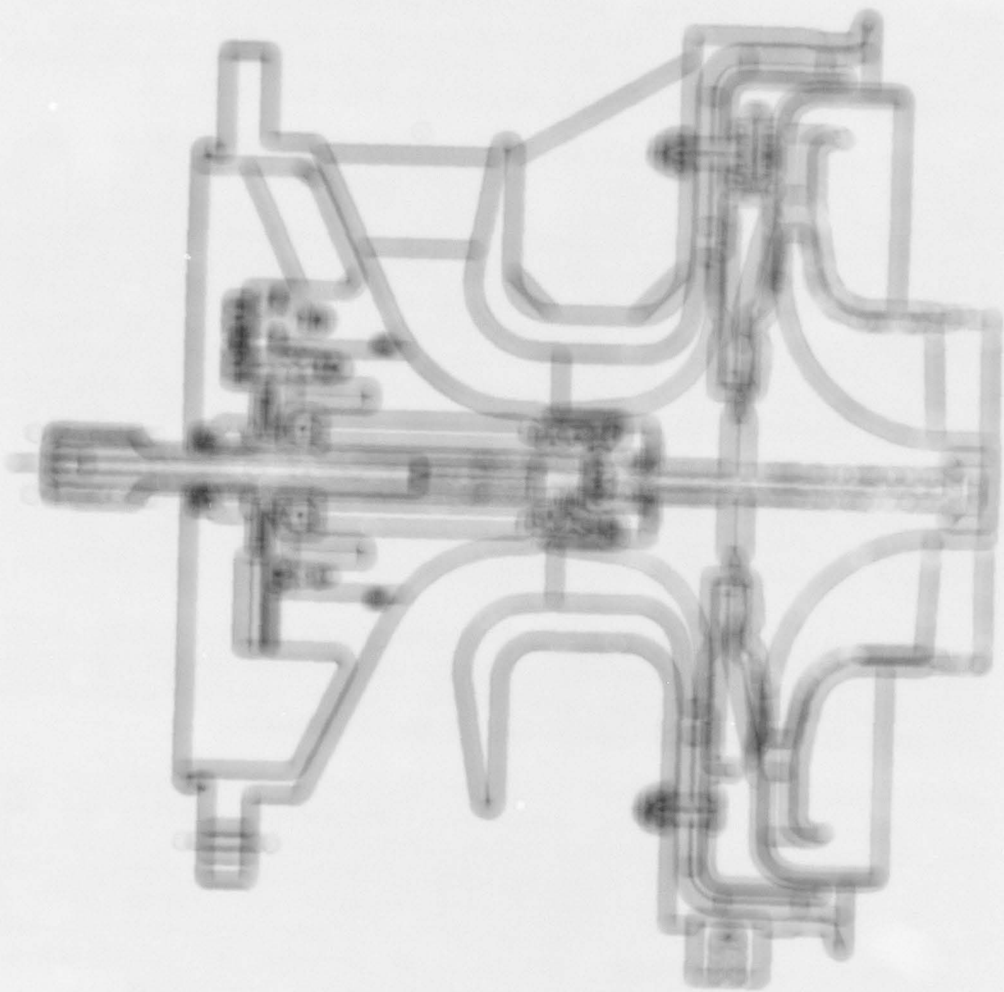

Figure 5. Engine Test Rig (Turbine Cross Section)

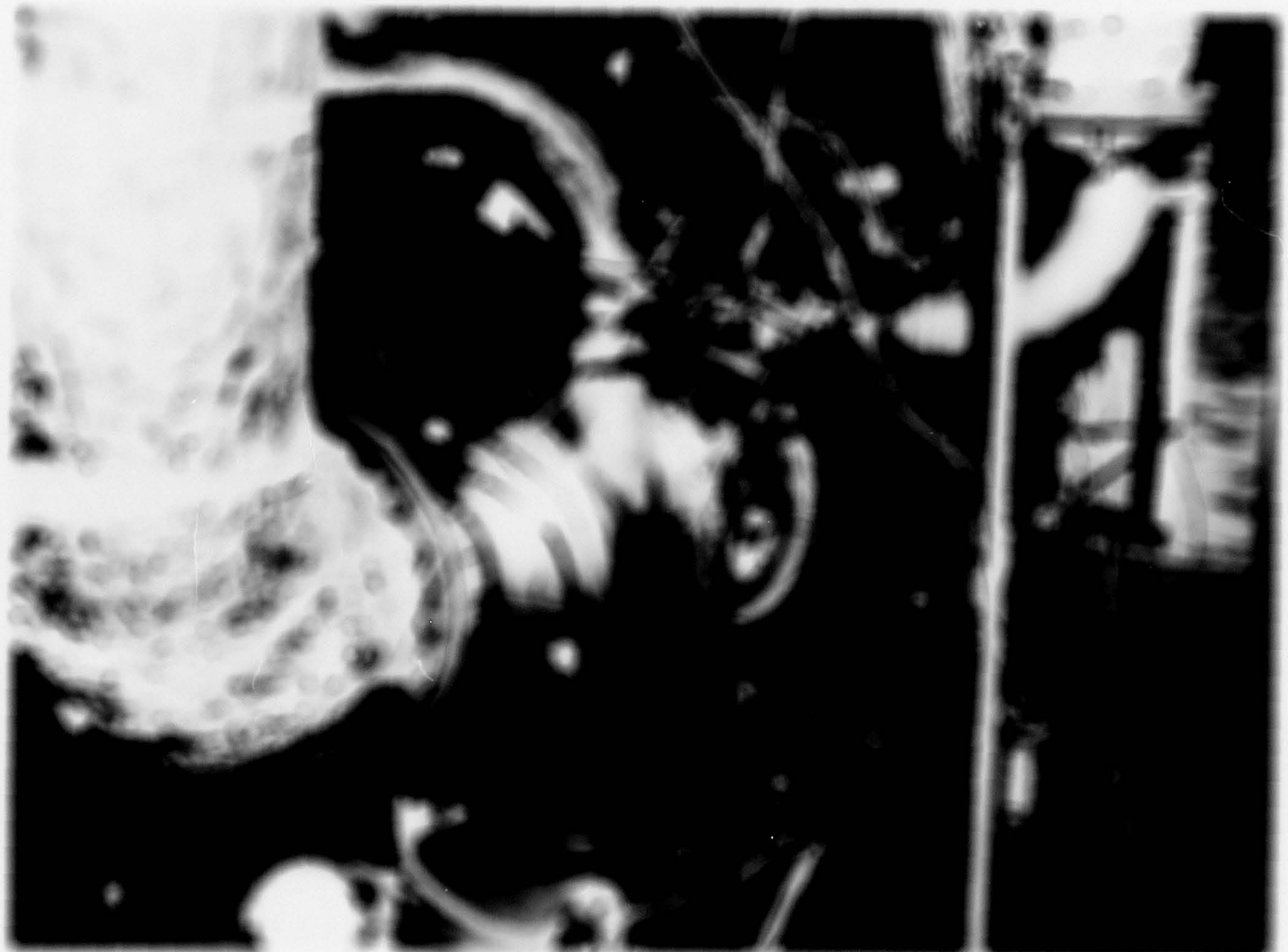

Figure 5. Compressor Test Rig

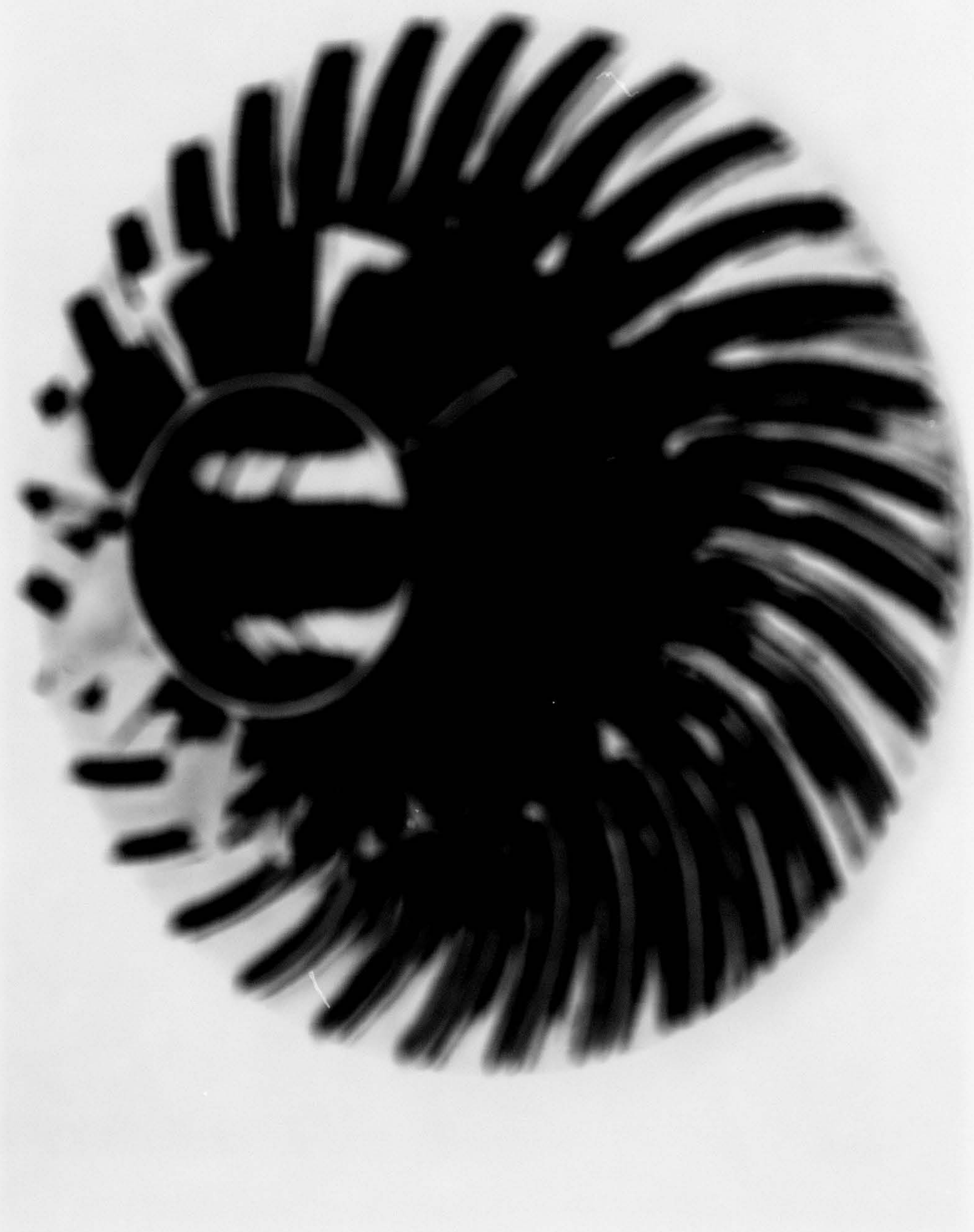

Figure [illegible]. [illegible] Compressor

Table 2

Compressor Major Aerodynamic Performance Parameters, [illegible]

[illegible] (deg)	[illegible]
[illegible] Speed (rpm)	[illegible]
Airflow [illegible]	[illegible]
[illegible] Tip Diameter (in.)	[illegible]
[illegible] Tip [illegible]	[illegible]
[illegible] Blade Angle (deg)	[illegible]
Impeller Tip Diameter (in.)	[illegible]
Impeller Tip Blade Angle (deg)	[illegible]
Impeller Tip [illegible]	[illegible]
Impeller Tip Speed (ft per sec)	[illegible]
Impeller Tip Width (in.)	[illegible]
Impeller Tip Clearance (in.)	[illegible]
Diffuser [illegible] Diameter (in.)	[illegible]
Diffuser [illegible]	[illegible]
Diffuser [illegible] Ratio	[illegible]
Diffuser Vane [illegible] (in.)	[illegible]
Diffuser Exit Diameter (in.)	[illegible]
Overall Efficiency (%)	[illegible]
Pressure Ratio	[illegible]
Specific Speed	[illegible]
Work Factor	[illegible]

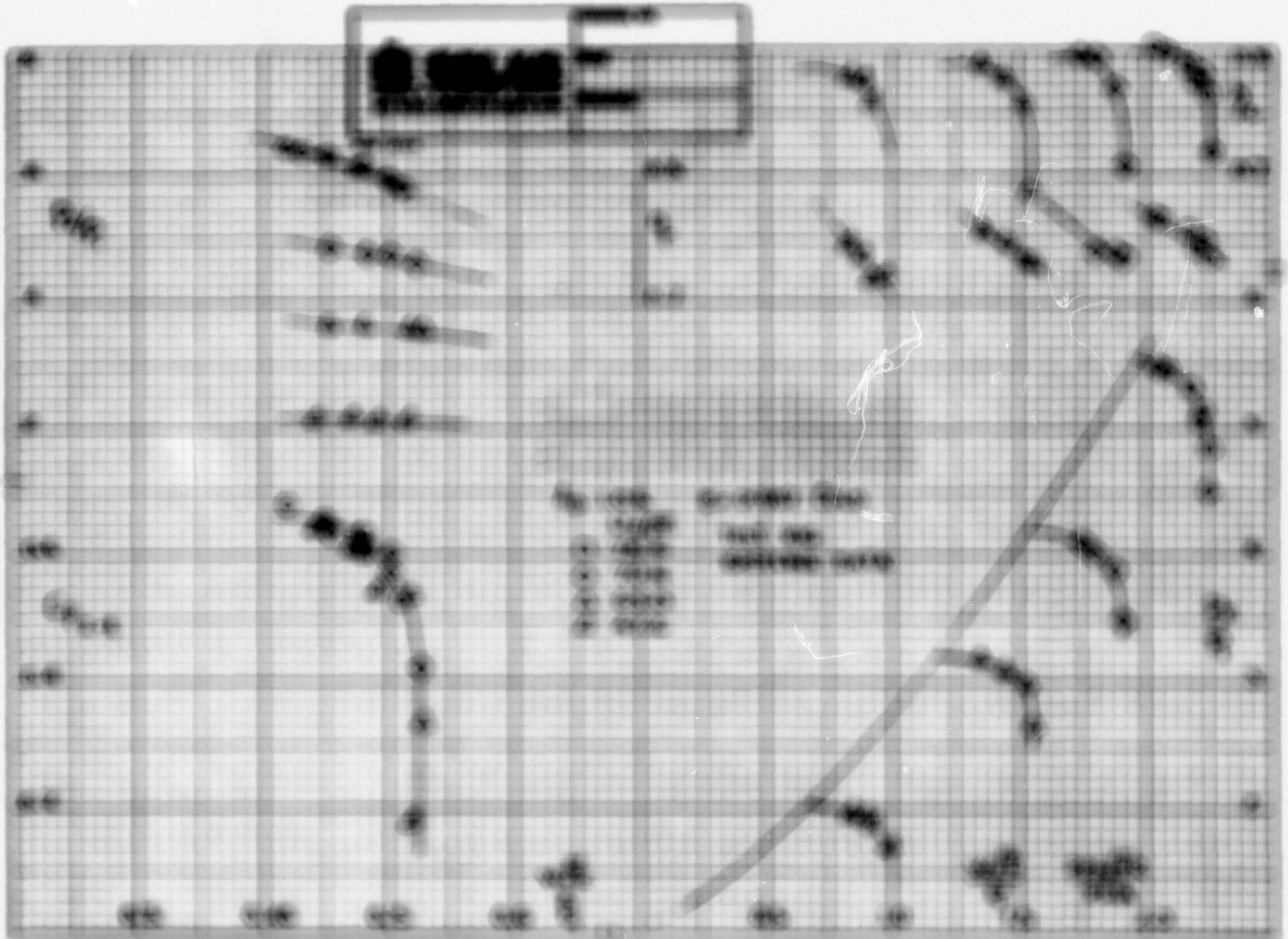

Figure [illegible]. Rig Test Compressor Performance

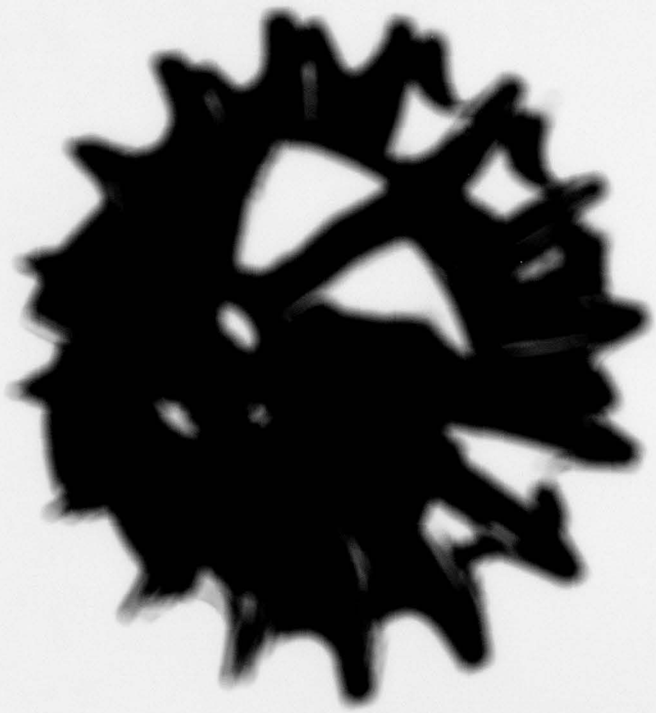

[illegible]

[illegible] Critical Speed Analysis. [illegible]

	Compressor	Turbine
Weight (lb)	[illegible]	[illegible]
Polar Moment of Inertia (lb in. sec^2)	[illegible]	[illegible]
Diametral Moment of Inertia (lb in. sec^2)	[illegible]	[illegible]

[illegible]

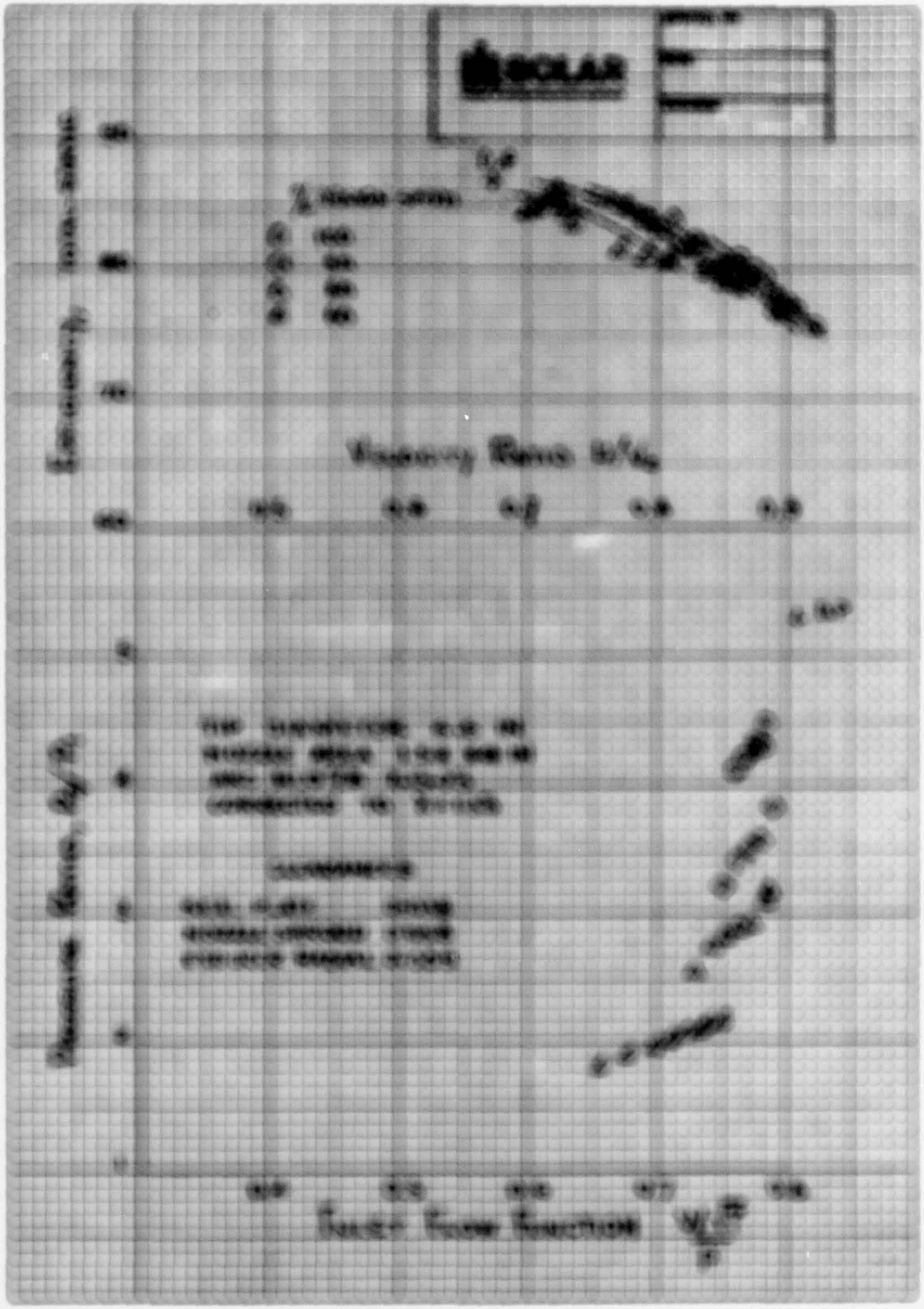

Figure 5. Turbine Rig Performance

Table II.

Turbine Major Aerodynamic Performance Parameters

Inlet Temperature (°F)	1860
Inlet Pressure (psi)	78
Pressure Ratio	5.3
Rotational Speed (rpm)	72,000
Nozzle Entry Diameter (in.)	9.0
Nozzle Exit Diameter (in.)	7.4
Number of Nozzles	23
Nozzle Width (in.)	0.29
Nozzle Throat Mach Number	0.89
Rotor Tip Diameter (in.)	6.5
Rotor Tip Speed (fps)	2042
Rotor Tip Width (in.)	0.32
Rotor Tip Clearance (in.)	0.02
Rotor Tip Mach Number	1.076
Reaction	0.44
Exducer Tip Diameter (in.)	4.25
Exducer RMS Blade Angle (deg)	40
Exducer Leaving Absolute Velocity (fps)	345
Total-to-Total Efficiency (%)	88.6
Total-to-Static Efficiency (%)	85.7
Inlet Flow (pps)	1.15
Specific Speed	72.2

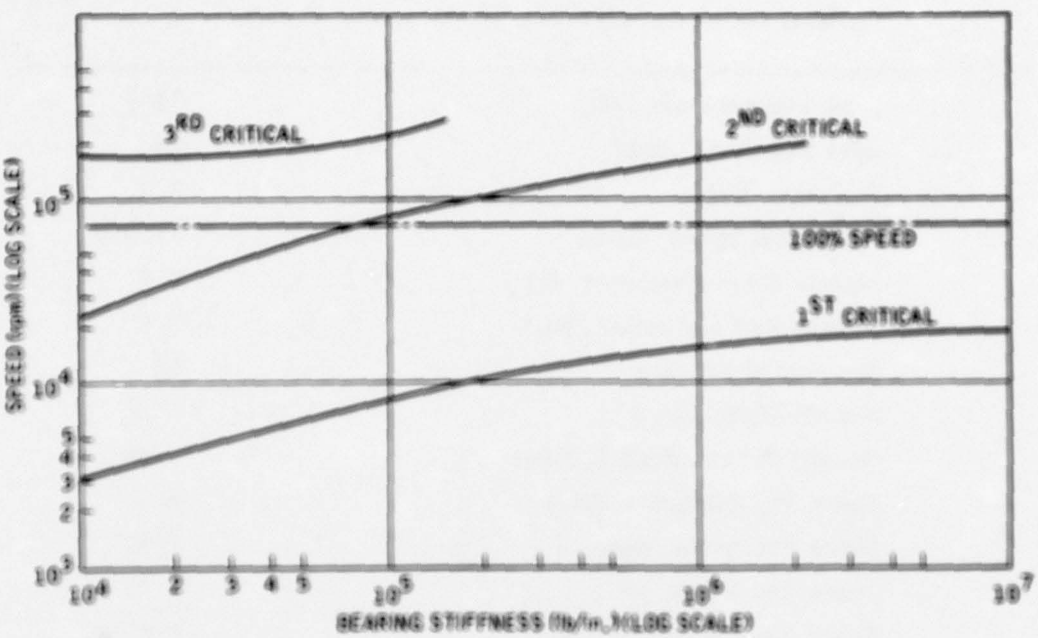

Figure 8. Engine Critical Speeds

The use of rigidly mounted and oil-dampened bearing systems operating in an out-of-balance condition showed, in a comparative investigation, that the response through the critical speed was sharper and of a higher level for the rigidly mounted system; however, the resulting bearing loads were well within the capabilities of the bearings considered. Estimated peak radial excursion of the turbine exducer tip through the critical speed was 0.007 inch, compared with an anticipated radial clearance of the order of 0.020 to 0.030 inch.

2.2.4 Rotor Bearing and Lube System Design. The rotor shaft and bearing configuration is typical of standard Solar "Titan" engines, using a roller bearing mounted inside the "eye" of the compressor as the primary radial support for the rotor and a ball bearing in the forward end of the housing for thrust loads. The rotor shaft is hollow, permitting air/oil mist from the reduction drive assembly to pass through the pinion and shaft, around the roller bearing, through the ball bearing, and back into the gearbox by a slinger nut, which acts as a centrifugal impeller. This mist is augmented by oil injection from a jet which directs a metered quantity of oil into the hollow end of the drive pinion, which can be seen in the turbine assembly cross section in Figure 2. The rotor bearings are supported in a bearing capsule, also shown in Figure 2.

The capsule itself is shown in Figure 9, and the turbine rotor, the bearing capsule, and the pinion are shown as an assembly in Figure 10.

The assembly of the rotor system into the air inlet housing is shown in Figure 17.

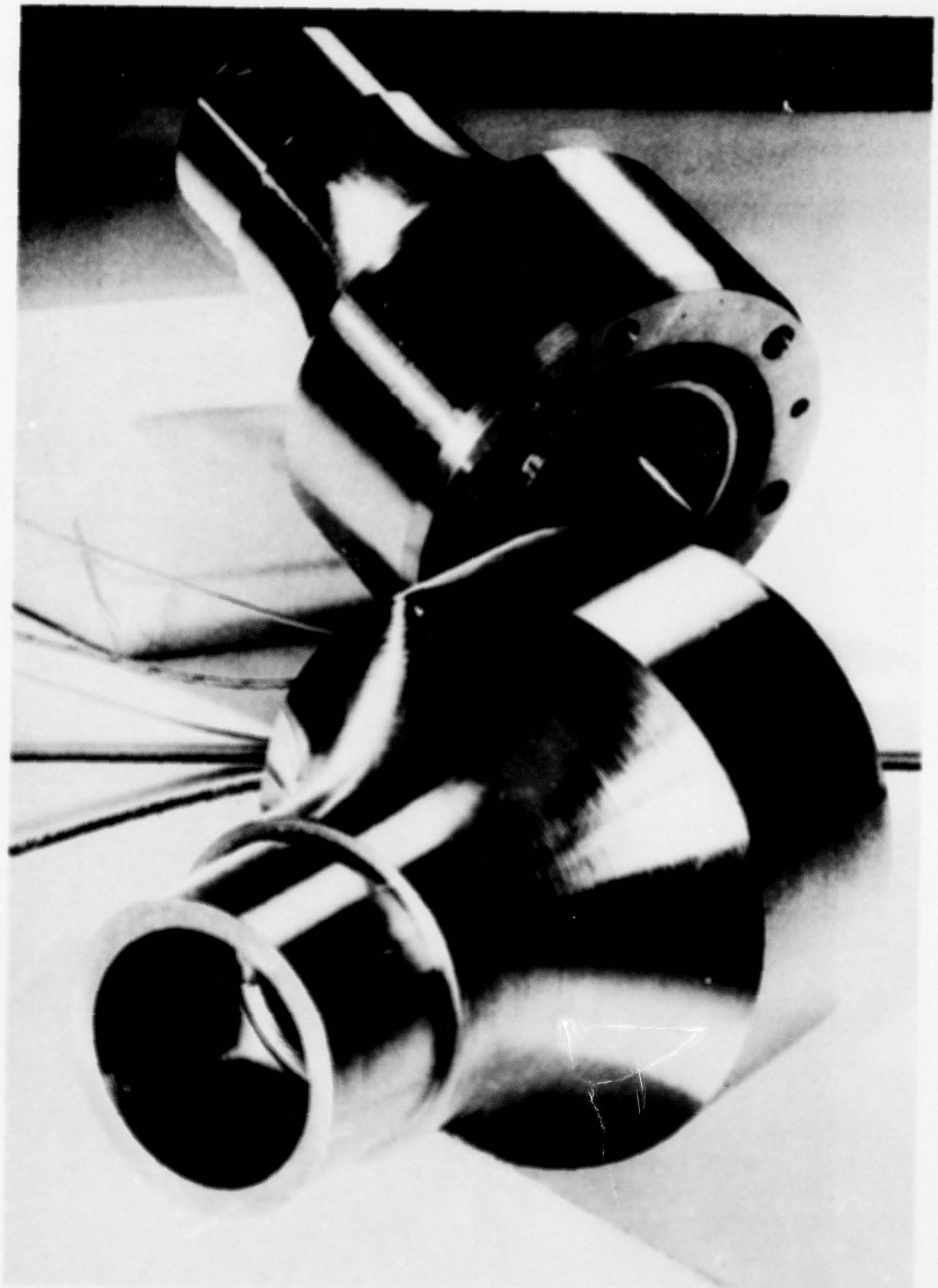

Figure 9. Instrumented Rotor Bearing Capsules

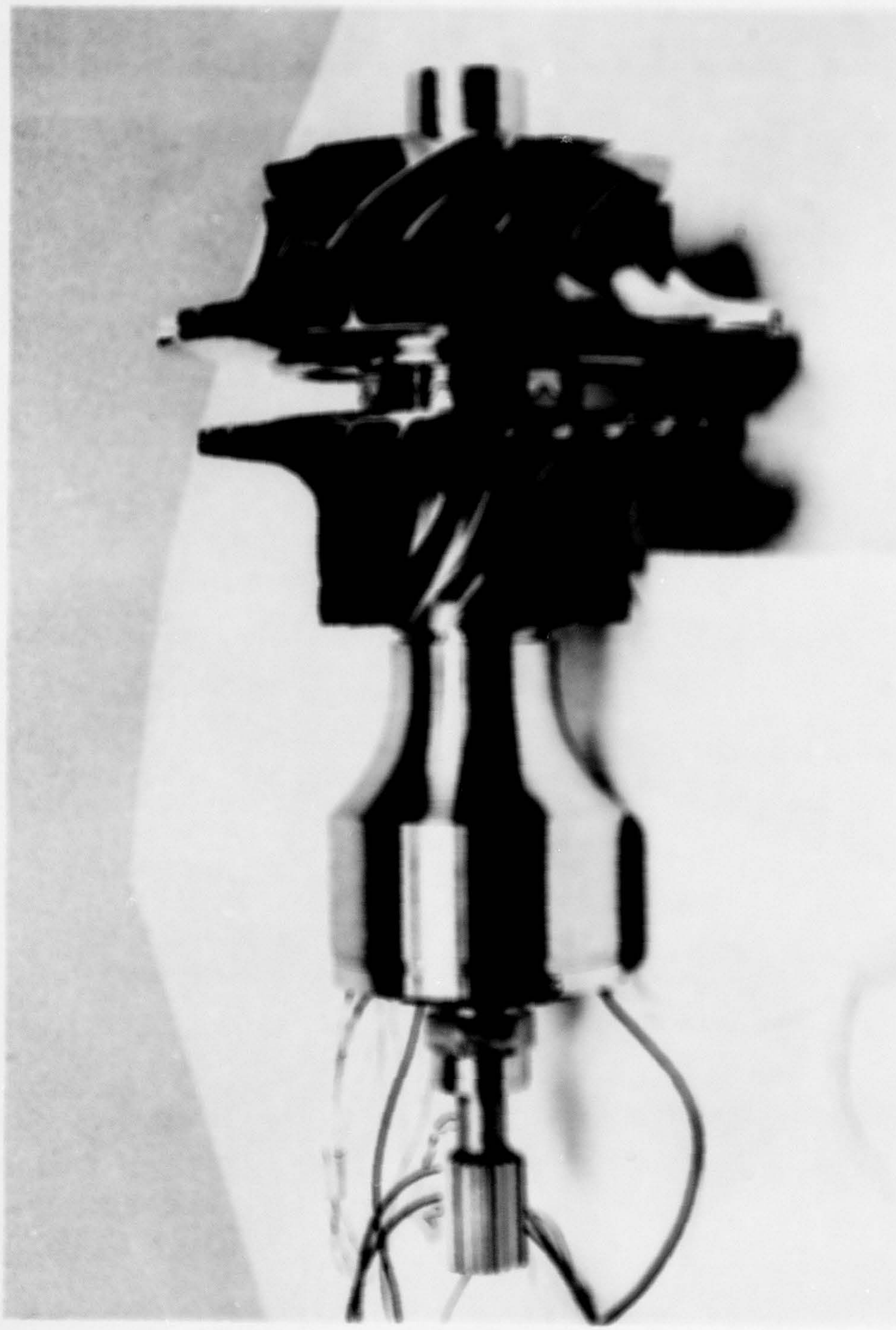

Figure 10. Turbine Rotor, Bore up Cupola, and Piston Assembly

The design requirement for the bearing system was a B10 life of 8000 hours at the rated speed of 75,000 rpm. Under this condition it was recognized early that the rotating assembly axial thrust would be of major importance and that efforts to optimize the thrust, either mechanically or aerodynamically, would significantly assist in meeting the design requirements.

Although excessive axial load imposed on the thrust bearing balls increases stresses and reduces life, a minimum load level is required to prevent ball skidding. The thrust bearing must have sufficient axial load at all times to keep the balls tracking correctly. An axial load of 75 pounds was calculated as the minimum necessary to prevent the occurrence of skidding.

To calculate bearing life it was necessary to estimate rotating assembly aerodynamic axial thrust as governed basically by the compressor pressure ratio, floating design practices, and turbine rim scallop diameter. Figure 11 shows estimated axial net thrust at design speed and rated power output as a function of turbine rim scallop diameter, and indicates that a zero-thrust condition is possible with a full disc turbine rotor. Scalloping of the disc is necessary, however, to prevent high transitory thermal stresses capable of causing rim cracking.

Based upon experience with previous Titan turbine rotors, it was decided to select initially a scallop diameter of 5.9 inches with a resulting axial net thrust of 100 pounds at maximum output. Further thrust calculations at various engine load conditions showed that the average mission thrust over a typical load profile would be of the order of 100 pounds.

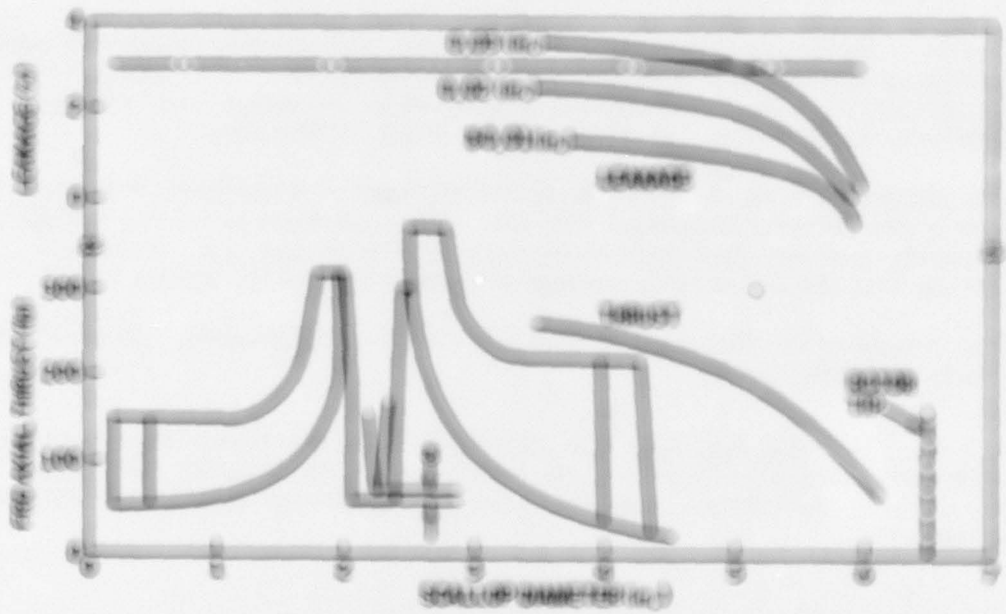

Figure 11. Engine Estimated Net Thrust

[illegible]

[illegible]

[illegible]

[illegible]

[illegible]

[illegible]

[illegible]

[illegible]

[illegible]

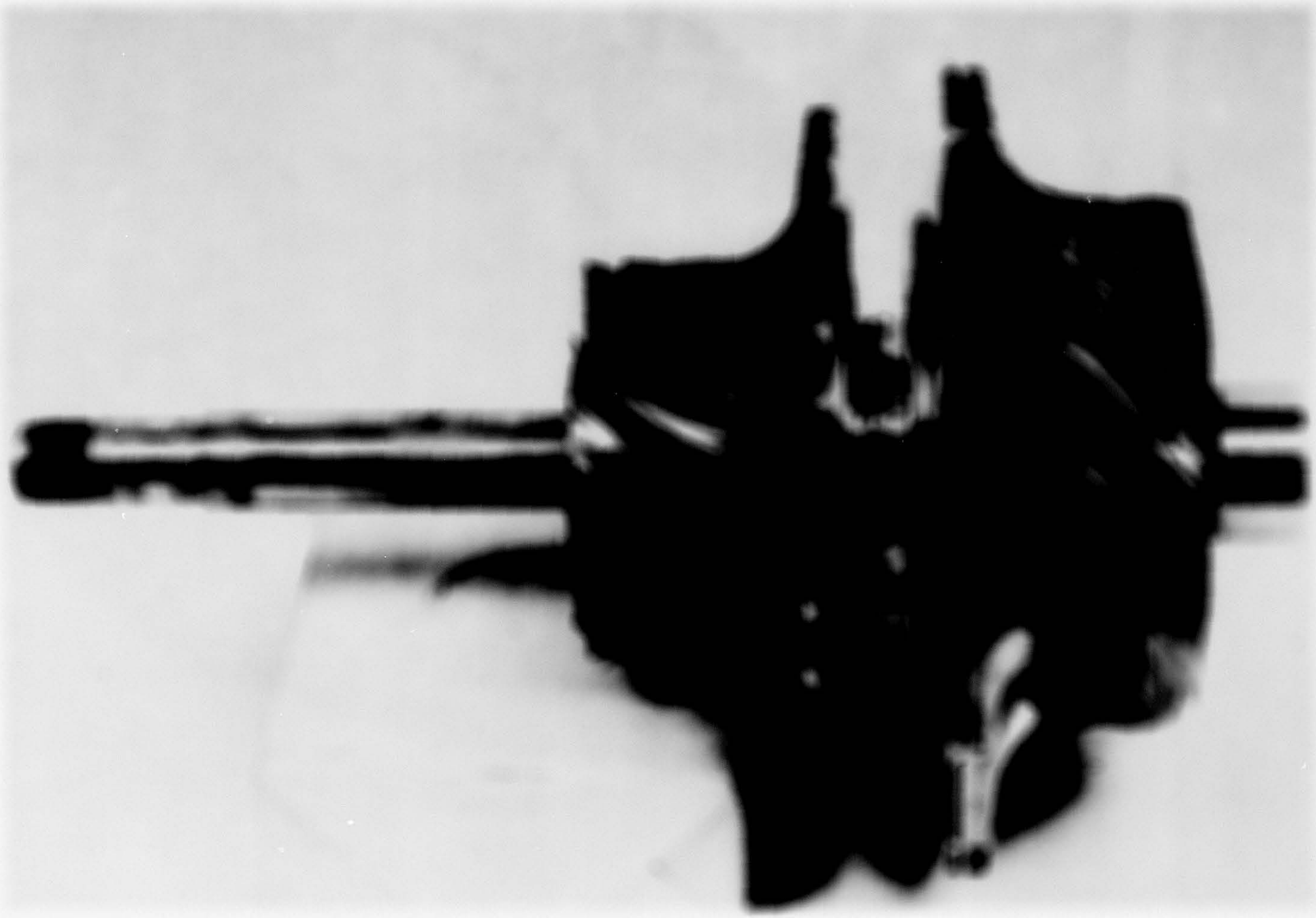

Figure [illegible]. Rotor Assembly Showing Curvic Coupling to Shaft

Figure 15. Compressor Curvic Coupling

Figure 16. Engine Big Seal Plate

The air inlet housing is shown in Figures 15 and 16. The inlet housing [illegible] supports the bearing support flange [illegible], which is shown [illegible] in Figure 17. The diffuser and turbine nozzle are located [illegible] and [illegible] by the air inlet housing assembly in such a way that the compressor and turbine [illegible], with clearances between the rotating and non-rotating parts of the engine designed for optimum overall performance.

5.5.8 Diffuser. The compressor diffuser is located inside the air inlet housing as shown in the engine rig cross section in Figure 5. The diffuser is a conventional channel-type design with a [illegible] vane [illegible] ratio for maximum recovery. The diffuser is also shown in Figure 18.

5.5.9 Turbine Nozzle. Figure 19 shows the turbine nozzle assembly that was designed specifically for the advanced [illegible] engine test rig, using a [illegible] [illegible] method.

Clamping bolts pass through the diffuser assembly and air inlet housing to provide axial location and support. The flange [illegible] [illegible] consideration would be [illegible] during thermal growth by the [illegible] [illegible] as shown in the photograph.

This arrangement was not satisfactory and design modifications were necessary during the development program, as discussed in Section 7.

5.5.10 Combustor Assembly. A slightly modified T-[illegible] Titan combustor completes the assembly and permits operation as a self-sustaining rig. The combustor receives air from the compressor and diffuser between the air inlet housing and liner walls. Primary combustion air is mixed with fuel in the injector [illegible] in the dome of the liner. The dome and liner walls are cooled by the introduction of compressor air through many [illegible] holes. Secondary or dilution air is admitted through a row of larger holes [illegible] along the combustor outer liner. The combustor assembly receives the discharge of airflow from the compressor/diffuser assembly and delivers the discharge from the combustor to the turbine nozzle assembly.

An external view of the engine rig combustor case assembly is shown in Figure 19. This photograph shows the bleed port, which permitted a wide range of compressor performance to be evaluated.

5.5.11 Fuel System. The fuel control was from a conventional Titan engine system but with a new acceleration fuel schedule, which was necessary to meet the fuel flow requirements of the advanced [illegible] engine test rig. Modifications were also necessary to allow steady-state operation at off-design speeds for compressor mapping.

The fuel distribution system, including fuel injection into the combustor assembly, was essentially the Titan T-[illegible] configuration.

Figure 15. LO Side Housing and Stator Coupler Retaining Plate

Figure 16c. Air-Side Housing and Compressor Diffuser

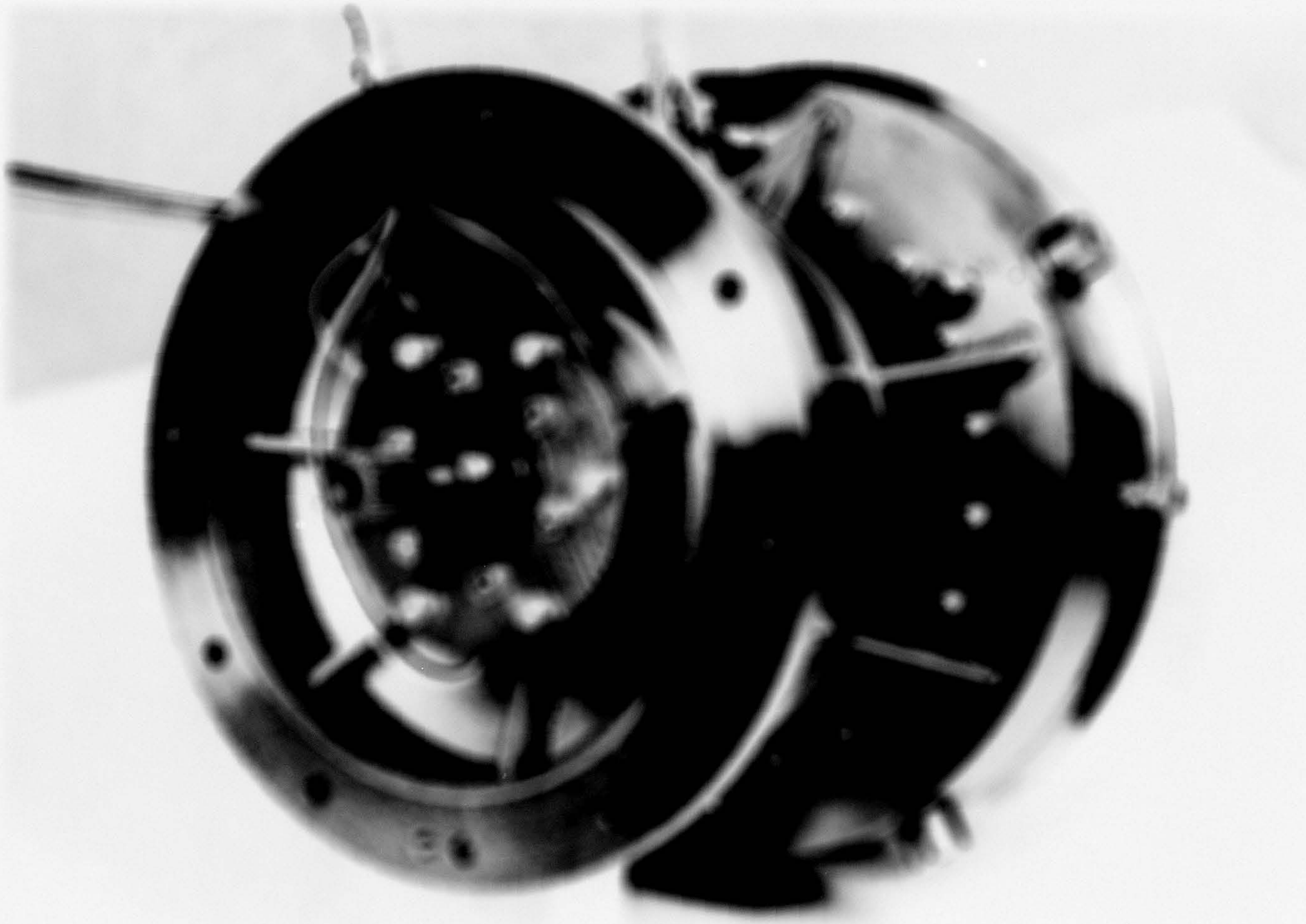

Figure 15. Air Side Housing with Turbine Assembly Installed (Front View)

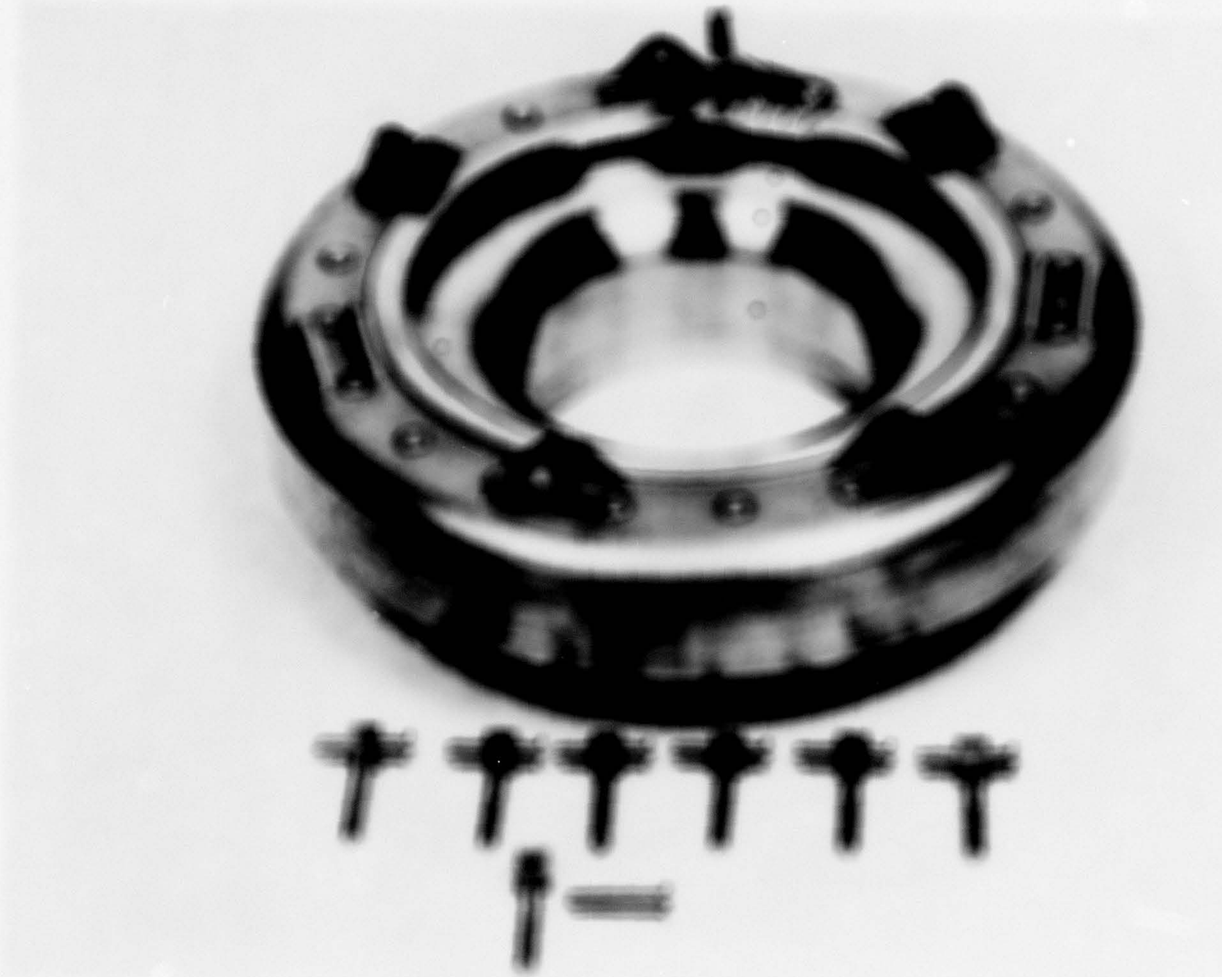

Figure [illegible]. Turbine Nozzle Assembly

Figure 16. Combustion Housing

3

ENGINE TEST RIG

The design of the engine test rig allowed for the disassembly and reassembly of the turbine wheel, turbine nozzle, and seal plate without disassembling or affecting the remaining engine/rig. Thus, the turbine wheel/turbine shroud seal plate clearances could be varied while the engine/rig remained on the test stand.

The engine test rig incorporated a standard T-62T-32 engine reduction gearbox and a facility water dynamometer. Also, the engine test rig combustor housing incorporated a bleed port to allow compressor mapping over a broad range. The engine/rig was fitted with a modified Titan fuel control, which was manually controlled to allow engine test rig operation at various speeds and loads.

3.1 DESCRIPTION OF INSTALLATION

All testing of the engine test rig was conducted in the development test cell facility at Solar Division of International Harvester. A schematic of the test cell setup is shown in Figure 20.

A 150-horsepower, 6000-rpm facility water dynamometer was used to measure the engine test rig shaft power output. The compressor inlet air was drawn from the cell while the turbine exhaust gas and the compressor discharge bleed air was ducted outside the cell.

The engine test rig used JP-4 fuel from the facility supply system and MIL-L-7808 lubrication oil.

Figure 21 shows the instrumented engine test rig installed in the test cell.

3.2 INSTRUMENTATION

The engine test rig was fully instrumented to determine the overall and component aerodynamic performances. Figures 22, 23, 24, 25 and 26 show the location and installation details of pressure and temperature instrumentation. Additional instrumentation monitored the mechanical operation of the rig. Figure 28 shows the location of rub rivets that were installed in the turbine shroud and seal plate to determine the running clearances with the turbine wheel during operation. Special attention was given to the measurement of aerodynamic thrust loads on the turbine rotor caused by changes in operating conditions and by changes in the turbine wheel rim sealing configurations. A bearing retainer plate was modified with three strain gages, and their output leads were connected to a calibrated bridge to provide a direct rotor thrust measuring device. Table III

lists the aerodynamic and mechanical instrumentation that was used. In addition to the instrumentation listed, Spectral Dynamics analyzers available in the development test cells were used during the mechanical checkout of the system.

The pressures and temperatures used to calculate the aerodynamic performance of the engine test rig were scanned and recorded automatically by a facility data acquisition system (DAS). Selected pressures and temperatures were displayed independently to permit verification of the DAS operation and to facilitate field plotting of the data. The DAS will scan up to 48 pressures and temperatures and will print out its measurements in engineering units. The temperatures were sensed by a mix of resistance temperature and thermocouple probes. One scanning cycle of the DAS takes approximately 60 seconds. The mechanical operation instrumentation readout was displayed independently and recorded manually.

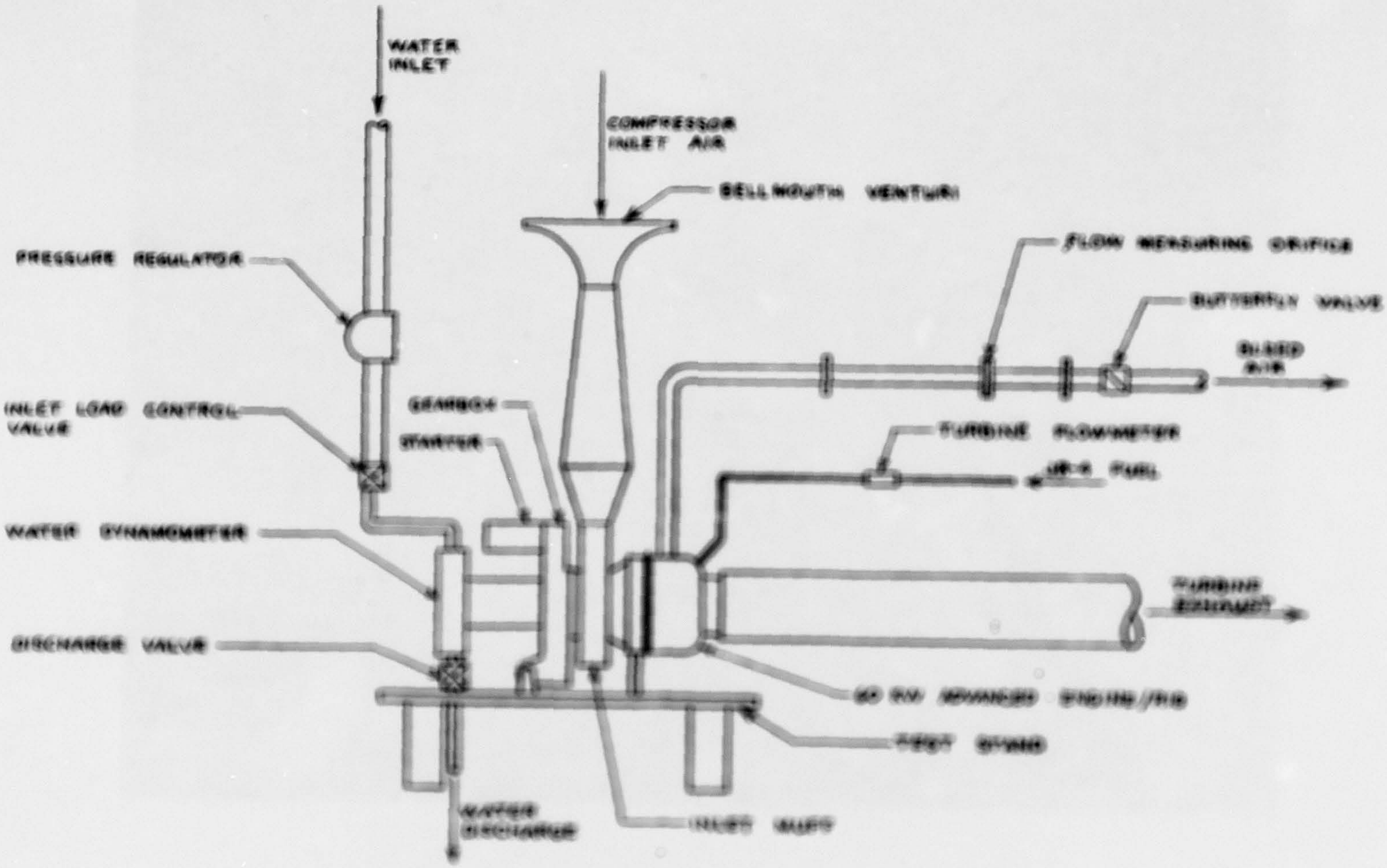

Figure 10. Advanced 10-kW Engine Rig Test Cell Schematic

Figure 21. Aft View of [illegible] kW Engine Test Rig Installed in Test Cell

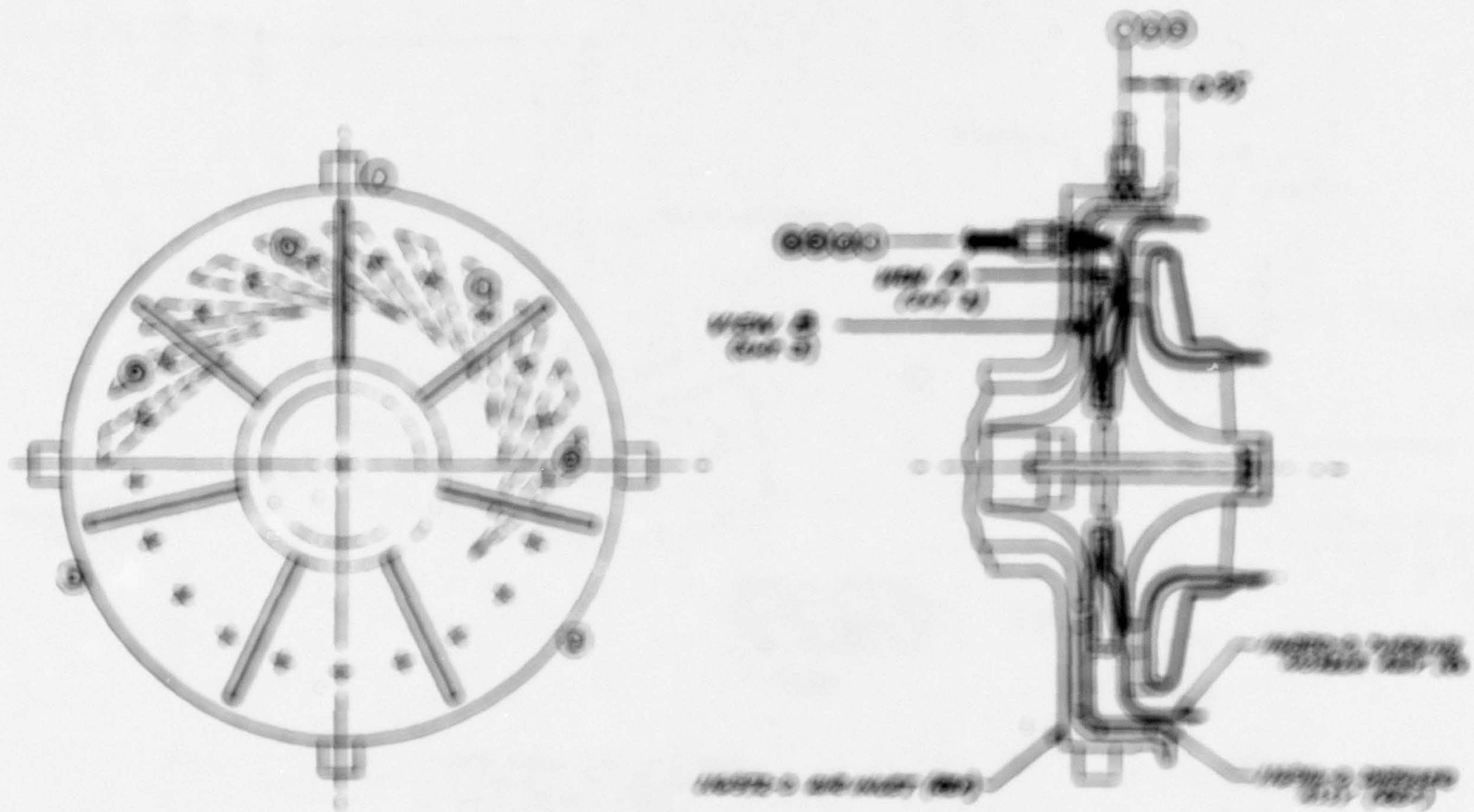

Figure 26. Power Turbine Section Pressure/Temperature Instrumentation

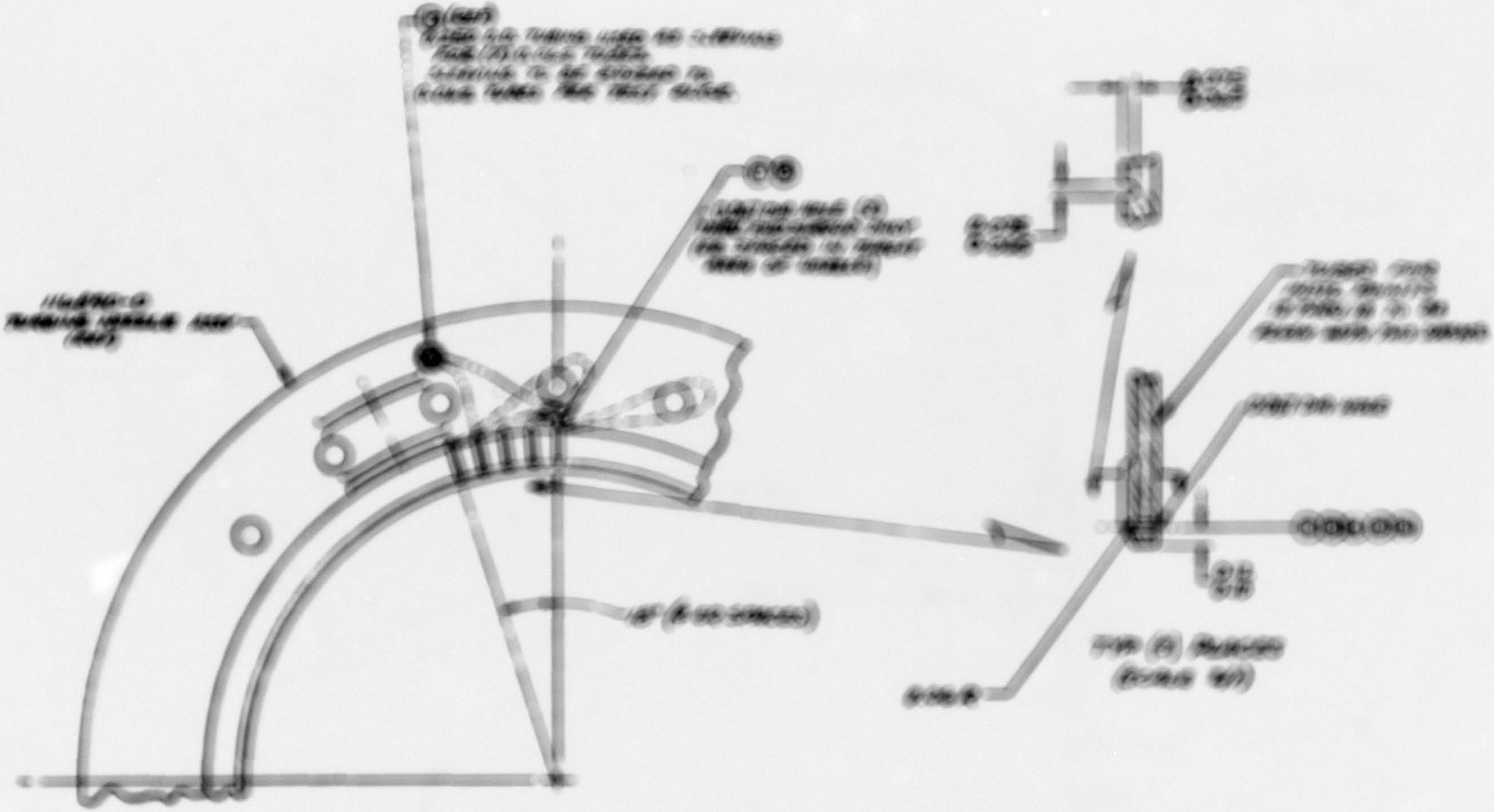

Figure [illegible]. Turbine Nozzle Pressure/Temperature Instrumentation

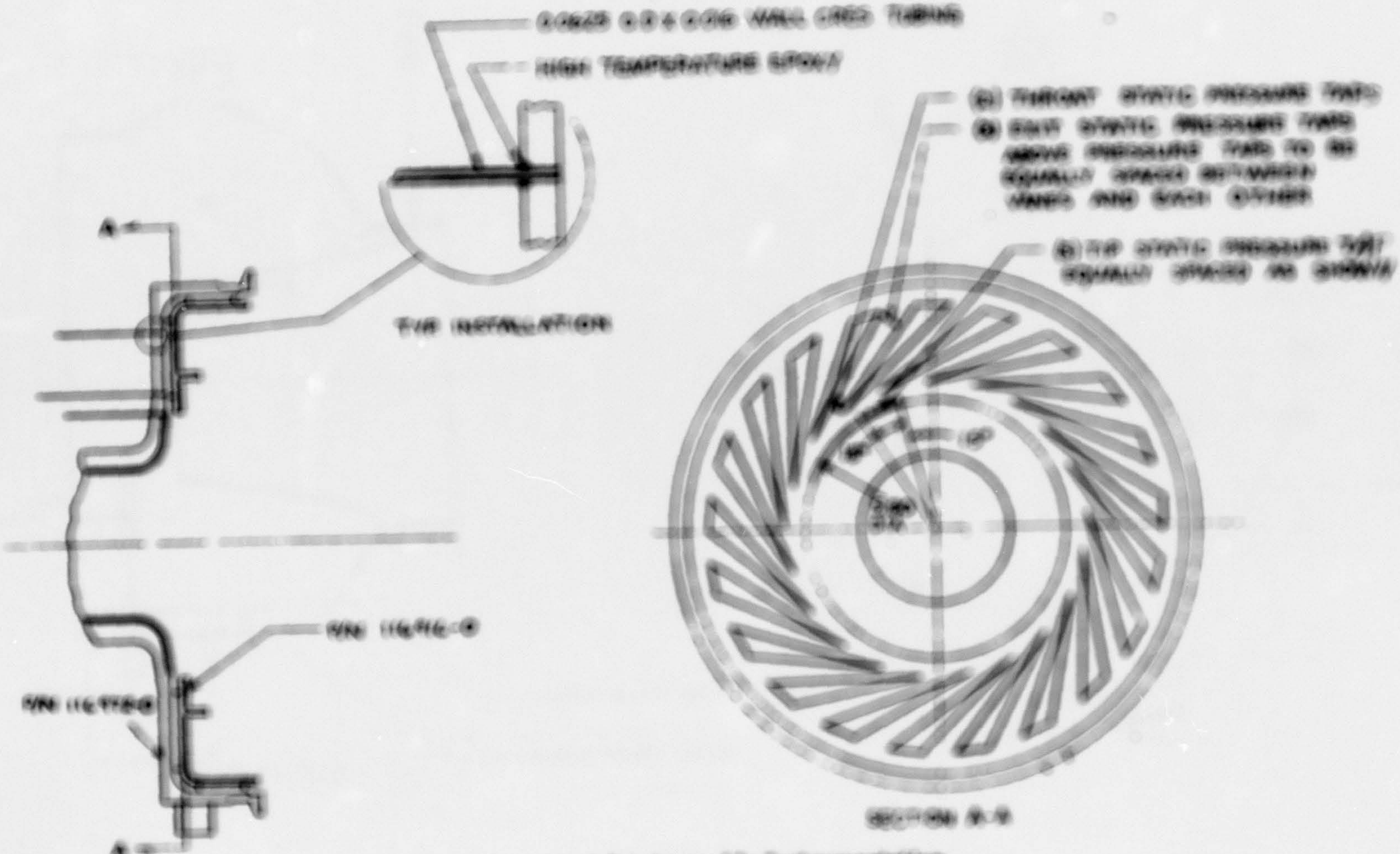

Figure 36. Air Inlet Assembly Instrumentation

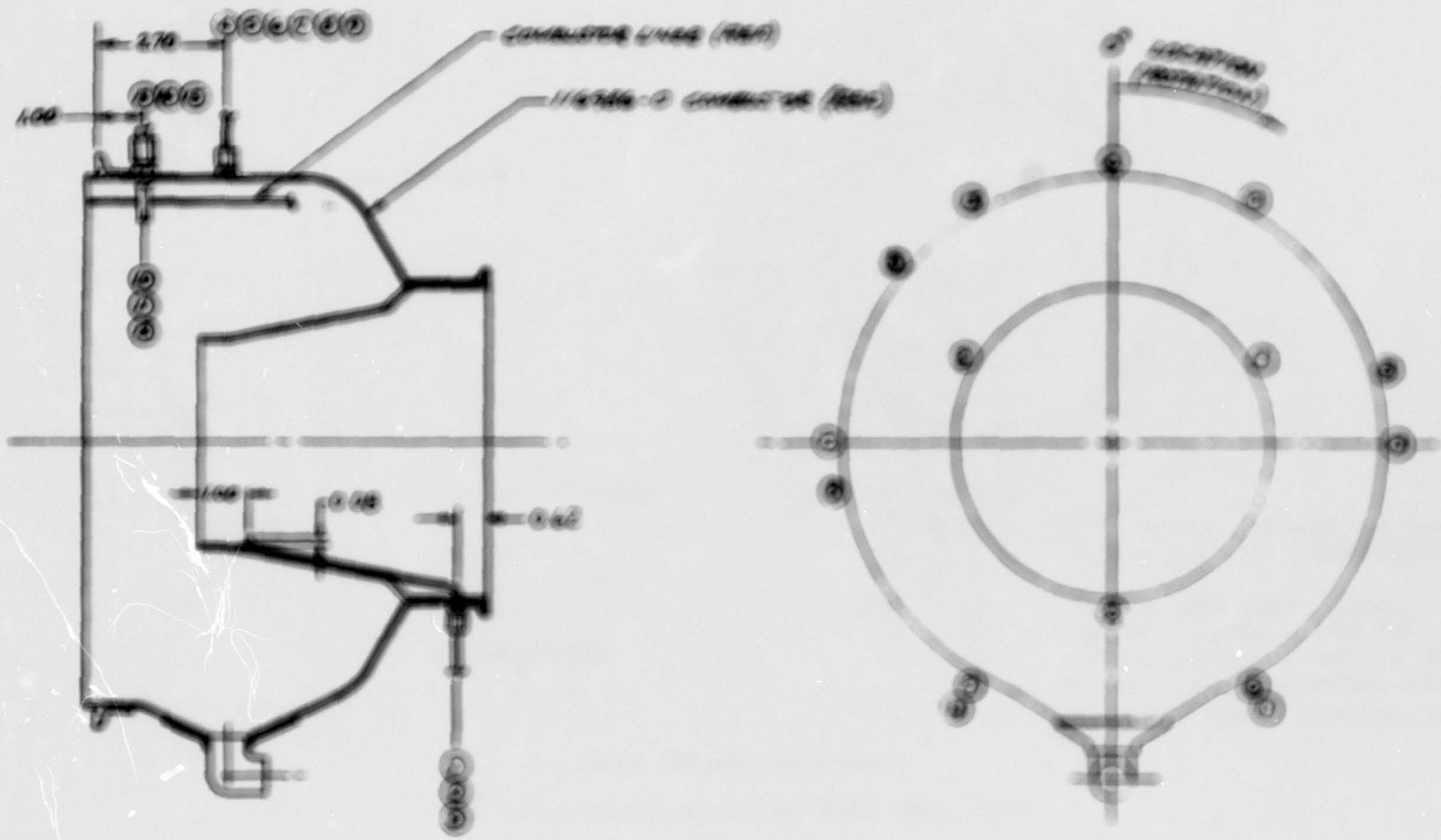

Figure 15. Combustor Assembly Instrumentation

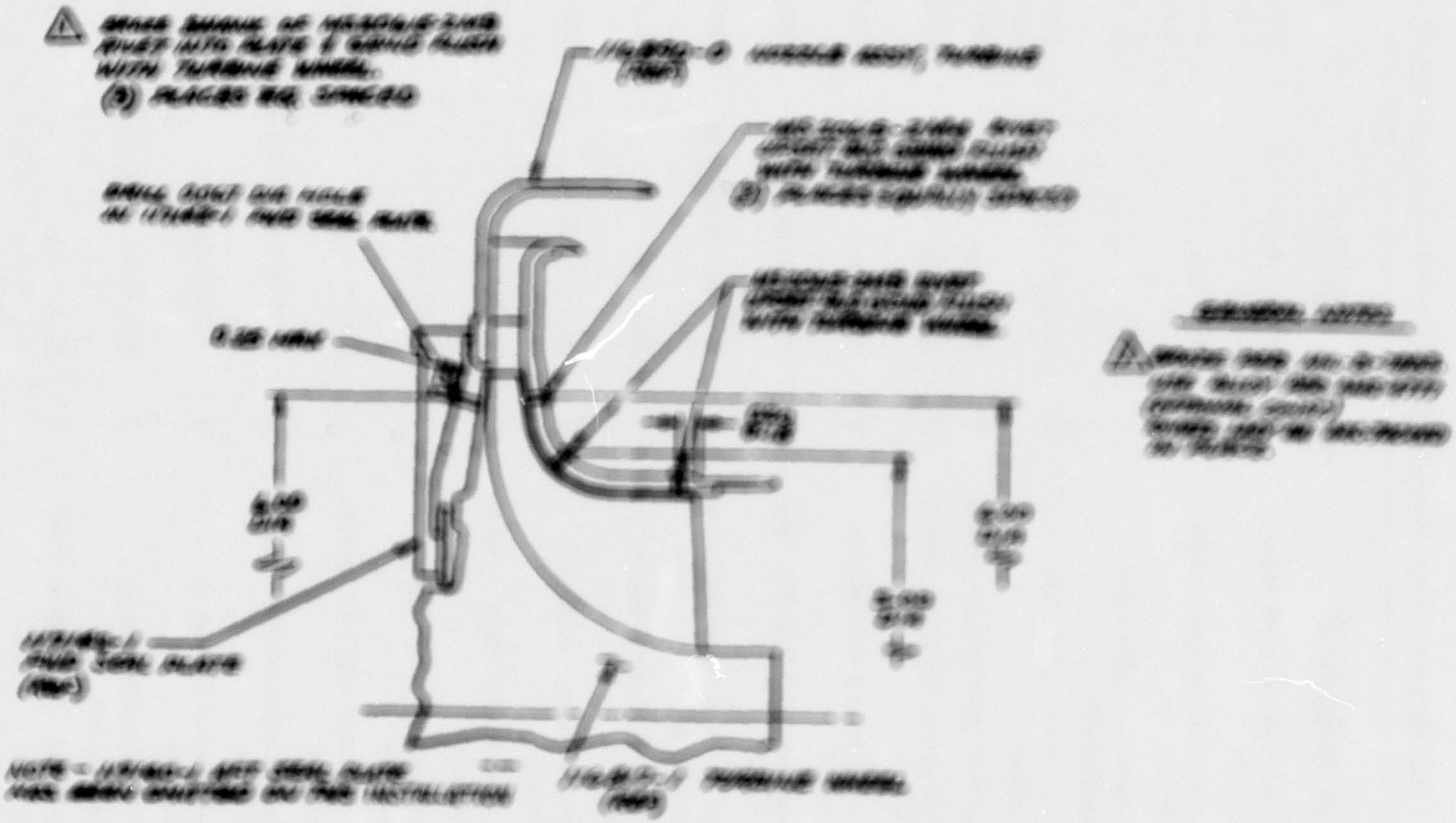

Figure 30. Turbine Nozzle Instrumentation

Table III.

Aerodynamic Performance and Mechanical Test Instrumentation

MEASUREMENT	NO.	SENSOR	READOUT
Engine venturi inlet temperature	1	RTD (resistance temp. device)	DAS (data acquisition system)
Engine inlet venturi throat pressure	3	Wall tap	DAS-3, H_2O manometer-3
Compressor inlet total temperature	6	RTD	DAS
Compressor inlet total pressure	6	Kiel probe	DAS-3, H_2O manometer-3
Impeller tip static pressure	5	Wall tap	DAS
Vaned diffuser throat static pressure	3	Wall tap	DAS
Vaned diffuser exit static pressure	3	Wall tap	DAS
Compressor discharge total pressure	3	Kiel probe	DAS-3, test gage-3
Compressor discharge total temperature	3	I/C thermocouples	DAS
Combustor scroll static pressure	6	Wall tap	DAS
Turbine nozzle inlet total pressure	3	Kiel probe	DAS-3, test gage-3
Turbine nozzle throat static pressure	2	Wall tap	DAS
Turbine rotor tip static pressure	5	Wall tap	DAS
Turbine diffuser exit static pressure	3	Static tap	DAS-3, H_2O manometer-3
Turbine exhaust total temperature	6	C/A thermocouples	DAS
Seal plate differential pressure	2	Static tap	DAS
Seal plate differential temperature	2	I/C thermocouples	DAS
Air bleed flow orifice inlet pressure	1	Static tap	DAS and test gage
Air bleed flow orifice discharge pressure	1	Static tap	DAS

Table III.

Aerodynamic Performance and Mechanical Test Instrumentation (Cont)

MEASUREMENT	NO.	SENSOR	READOUT
Air bleed flow orifice delta-P	2	Static tap	Hg manometer
Air bleed flow orifice total temperature	1	I/C thermocouple	DAS
Adapter bore static pressure	1	Static tap	DAS
Dynamometer load cell	1	Strain gage	Digital counter
Fuel flow	1	Turbine meter	Digital counter
Engine rpm	1	Mag. pickup probe	Digital counter
Lube oil inlet pressure	1	Static tap	Pressure gage
Lube oil sump temperature	1	I/C thermocouple	Digital counter
Radial vibration, engine	1	Accelerometer	Vibration meter
Horizontal vibration, gearbox	1	Accelerometer	Vibration meter
Bearing temperature	2	I/C thermocouple	Meter

4

DEVELOPMENT PROGRAM

The active portion of the development program began with receipt of the basic core components and assembly of the first engine test rig.

4.1 INITIAL BALANCE PROCEDURES

Rotor system balancing tests were conducted to determine the degree of repeatability obtainable using the turbine-to-compressor Curvic coupling. Different methods of simplifying the rotor balance technique were evaluated. A progressive balance procedure was used, starting with the rotor shaft and adding the compressor and the turbine wheel. Rotor component parts were indexed for minimum runout to the bearing journals.

Initial balance operation of the rotor shaft was straightforward. The rotor shaft was mounted on the balance machine at the shaft bearing journal locations, and balance material was removed to obtain balance within 0.001 ounce-inch in each correction plane. The compressor was installed on the rotor shaft, indexed, and the runout recorded. This assembly was mounted in the balance machine on the shaft bearing journals and balance corrections made to within 0.001 ounce-inch. Balance material was removed from the compressor only.

The turbine wheel was mounted and indexed to the rotor assembly for the least runout at the tip diameter with respect to the rotor shaft bearing journals. Attempts to balance the rotor system from the bearing diameters were unsatisfactory due to a lack of repeatability resulting from the short bearing span relative to the overhung turbine mass. This problem was eliminated by straddle-mounting the rotor assembly between the front bearing diameter and the turbine exducer outboard hub diameter in the balance machine. The degree of error introduced by this method is a function of the amount of runout measured at the turbine exducer relative to the bearing journals. The runout can be accurately controlled with future production design.

The turbine wheel was removed and reassembled to the rotor assembly to determine the degree of repeatability obtainable from the turbine-to-compressor Curvic coupling. The degree of residual imbalance of the rotor assembly remained well within the balance tolerance on three individual balance checks.

4.2 BLADE RESONANCE TESTS

Earlier tests on a related program had established that the compressor blades exhibited no resonances which would present a potential problem over the operating range of the engine test rig.

To preclude the possibility of fatigue failures on the turbine wheel blades, resonant frequencies were determined by "ringing" each blade. A microphone pickup and a frequency analyzer were used to detect and record the blade frequency. The blade fundamental frequencies were found to be grouped about [illegible] Hz. With a computed centrifugal stiffening effect of [illegible] percent, a possible interference with a second-order excitation at design speed was indicated. Since second-order excitation is always present, it was necessary to increase the blade resonant frequency; this was accomplished by "cropping" the exducer blade trailing edges by [illegible] inch axially at the O.D. and blending radially over a length of [illegible] inch. The turbine wheel blade resonant frequency was found to have increased to 2700 Hz. This modification placed the second-order excitation at [illegible] percent design speed, which was regarded as an acceptable safety margin.

6.3 ENGINE RIG ASSEMBLY

The rig was assembled to the clearance chart as shown on Figure 27 and the rig was delivered to test.

The clearance chart has been prepared with the objective of providing an easy reference for critical measurements on an assembly cell and as a record of each individual build-up dimension. Performance data obtained are cross-referenced to the engine build number so that later significant performance information can be related to aerodynamic clearances, etc.

In the Performance section of this report, several actual performance curves are plotted and the build numbers are identified in each case.

6.4 ROTOR EXCURSION MEASUREMENTS

Proximity probes were installed at the turbine wheel exducer outboard hub diameter to measure rotor excursions during initial rig cranking tests. The probes were held in position by a special fixture which was clamped to the outside diameter of the turbine nozzle exhaust (see Figure 28). Results of the cranking tests showed that the rotor system critical speed occurred at 8 to 10 percent rated speed, and that maximum peak-to-peak deflections in both horizontal and vertical planes were just less than 0.005 inch during passage through the critical speed.

Figure 29 shows an actual trace obtained from the instrumentation and plotted on a Spectral Analyzer.

The engine test rig operation under these cold-crank conditions was regarded as satisfactory, and the proximity fixture was removed.

A combustor was installed in preparation for mechanical shake-down operational tests.

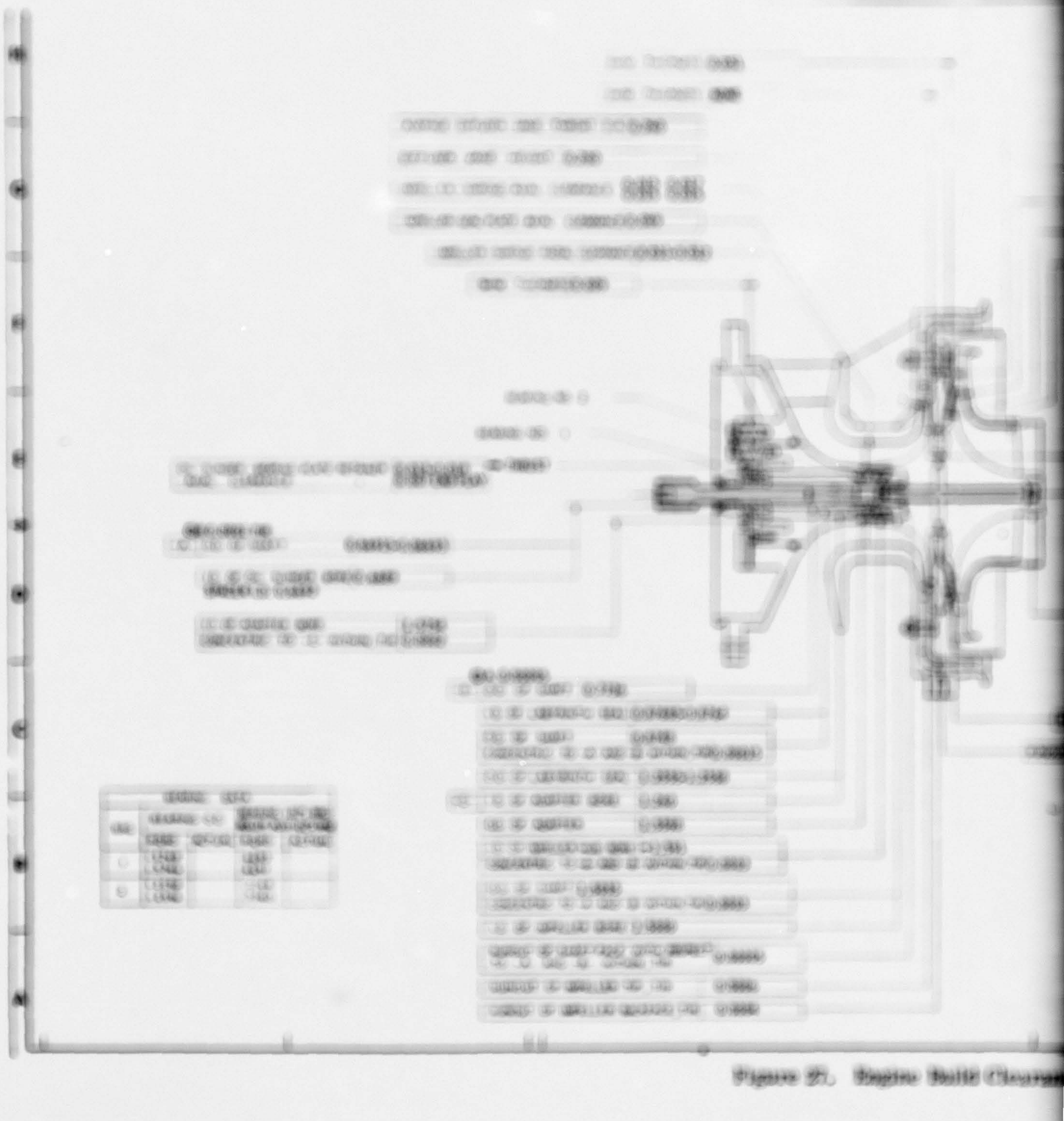

Figure 25. Engine Build Clearan

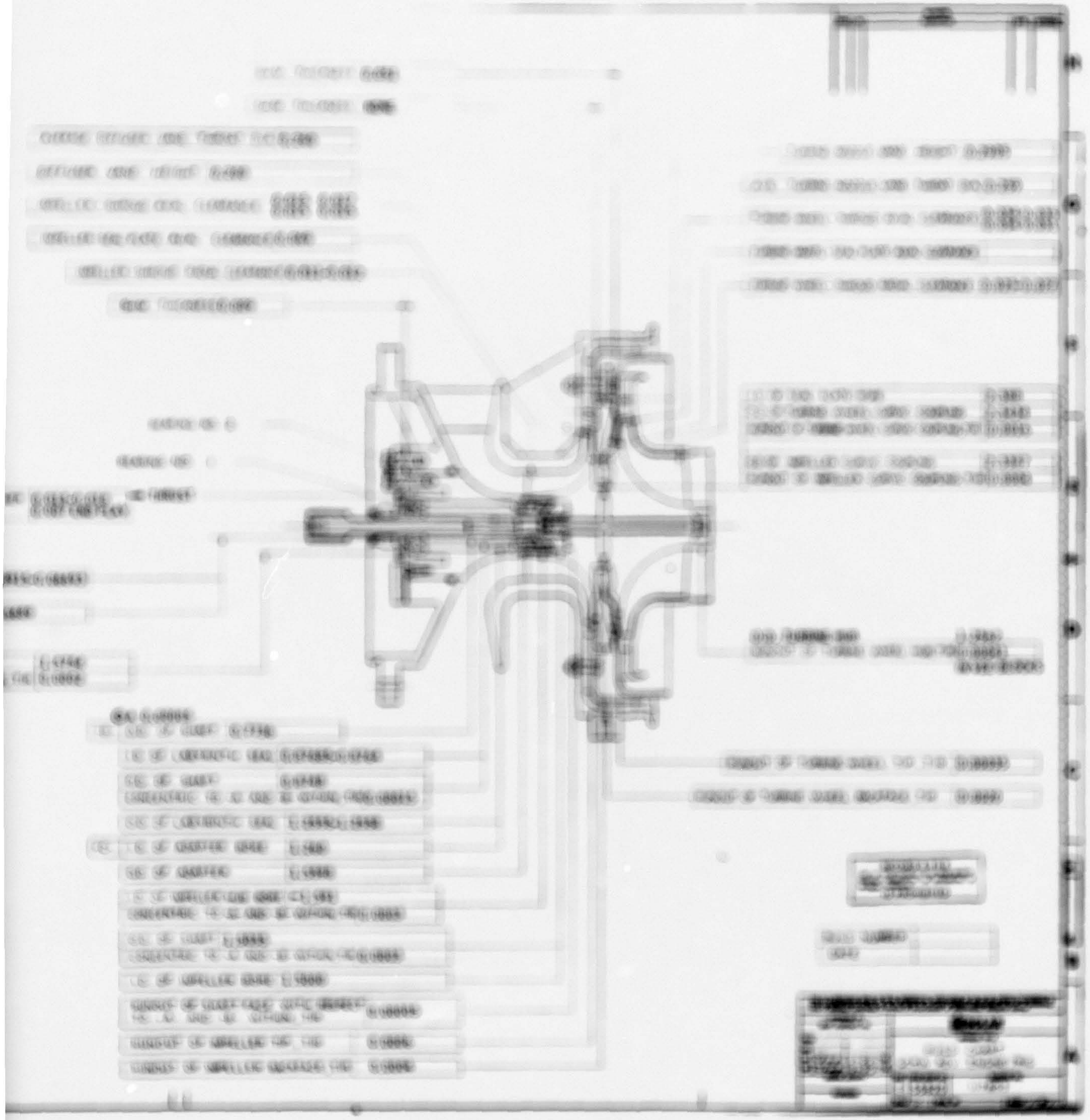

Figure [illegible]. Engine Build Clearance Chart

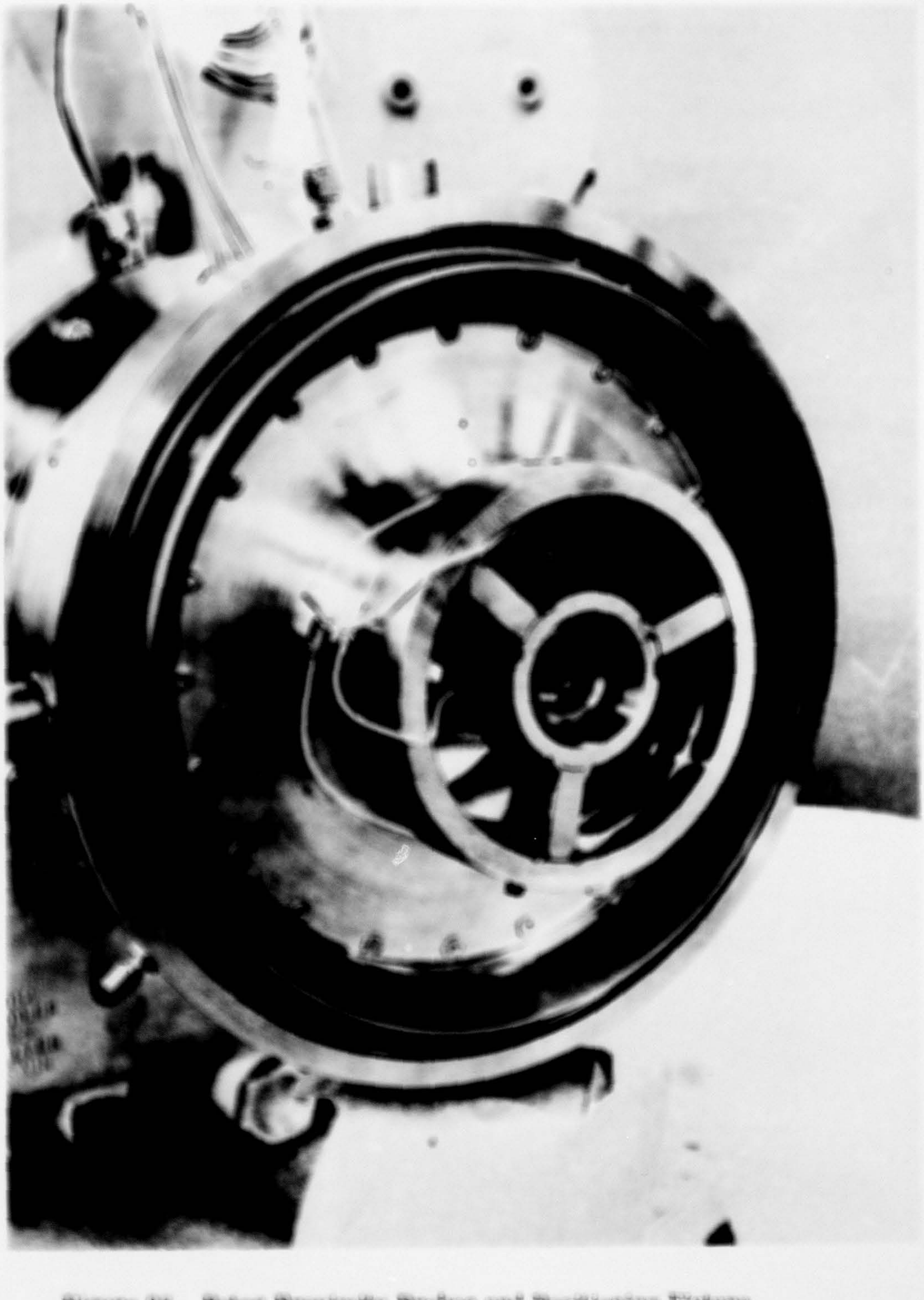

Figure 29. Rotor Proximity Probes and Positioning Fixture

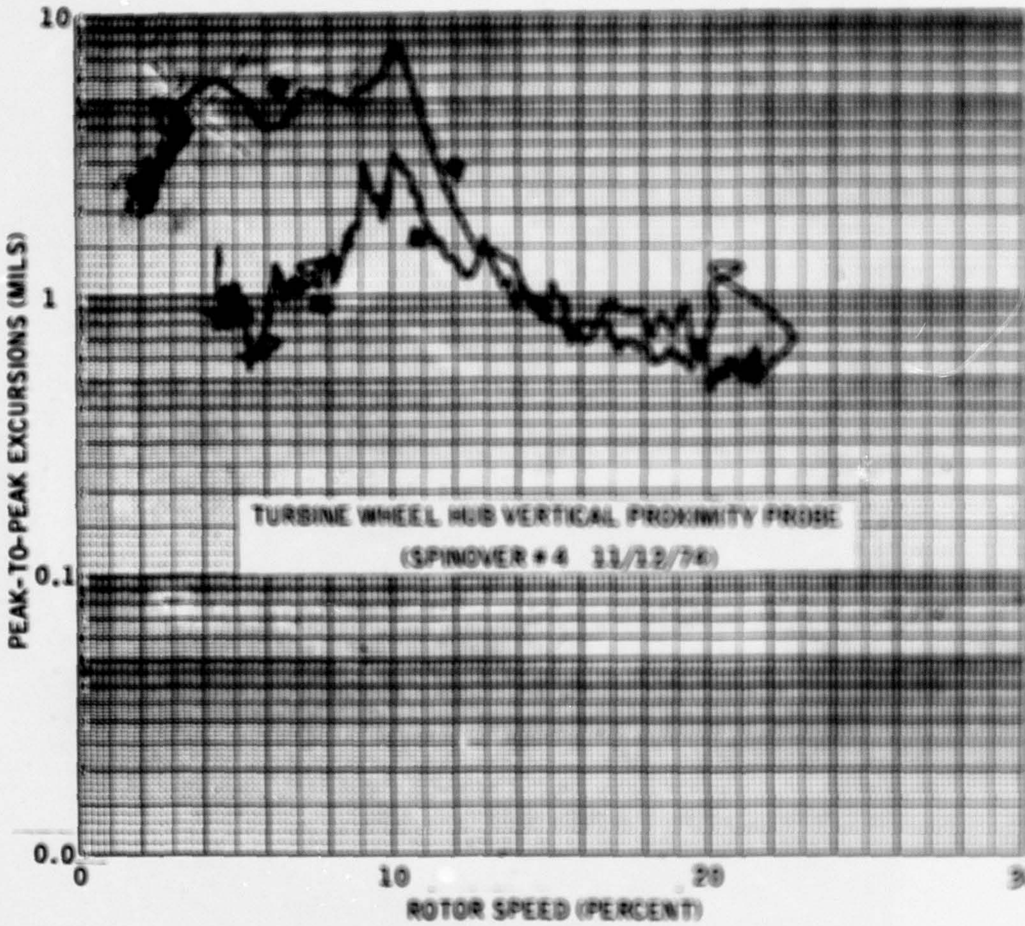

Figure 29. Spectral Analyzer Track of Rig Cranking Test

4.5 RIG OPERATIONAL TESTS

Early attempts to operate the engine/rig uncovered problems with mechanical rubs between the rotor assembly and the turbine nozzle. Repeated attempts to accelerate the rotor and to sustain intermediate speeds between 90 and 100 percent were unsuccessful.

It was established that the rotor rubs were not caused by high excursions resulting from a critical speed problem, because the problem occurred at various speeds in the 90 to 100 percent range approximately 2 to 3 minutes after stabilized running had been attained, indicating a thermal growth effect.

The conclusion was that the difficulties were caused either by component dimensional discrepancies or that the new design features, such as the method of retaining the turbine nozzle, were not performing as intended.

After several rig builds to correct minor discrepancies, replace damaged components, and to investigate minor design modifications, it was decided that the rotor rub problems were probably the result of a shift in the location of the turbine nozzle. A different method of positioning the nozzle was therefore introduced.

A 321 stainless steel piloting ring was bolted to the diffuser plate using the existing axial diffuser retaining bolts.

To investigate the problem further, proximity probes were reinstalled in two planes to measure rotor shaft mid-span excursions. An additional probe was incorporated in the air inlet housing to measure any motion of the bearing adapter relative to the housing.

The result of these tests was a confirmation that the rotor stability was not the basic cause of the contact between static and rotating parts.

Efforts were then directed towards a further reexamination of the methods used to pilot the static parts, particularly the turbine nozzle. It was decided to use radial pins through the air inlet housing, the diffuser assembly, and into the turbine nozzle in place of the original design shown in Figure 19. This new arrangement of nozzle locating pins is shown in Figure 30.

In addition, it was decided to eliminate the oil damping feature of the bearing capsule by adding three bolts through the air inlet to lock the capsule in place.

These changes were found to provide adequate control of the static components, and preliminary aerodynamic test data were recorded at a range of stabilized speeds.

Disassembly of the rig showed evidence of fret marks on the Curvic coupling, and it was concluded that the clamping torque of the turbine bolt had been too conservative. Bench tests showed that the torque could be doubled with an adequate safety margin, and the new higher torque was used on later rotor assemblies.

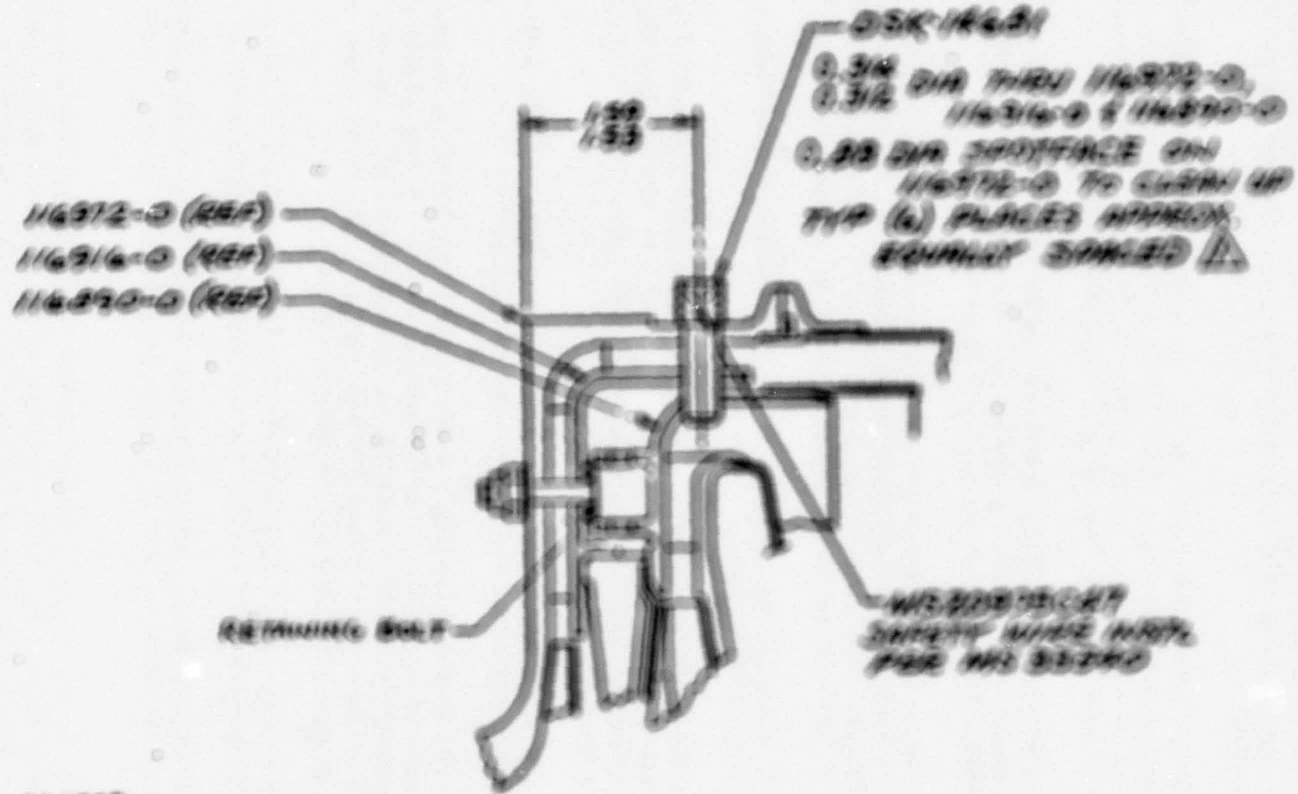

NOTES:
1. RADIAL LOCATION FOR PINS TO BE DETERMINED BY TEST ENGINEER.
2. FOR REMOVAL OF PINS (DSK 16681) AFTER TEST USE DSK 16680 EXTRACTOR & ALLEN WRENCH.

Figure 30. Conventional Nozzle Pinning Modification

The engine/rig was then reassembled and successfully tested at up to 100 percent speed (72,000 rpm). A full set of aerodynamic data was obtained at no load, partial load, and full load, which for this application was regarded as 80 hp (60-kW equivalent with a typical generator set).

The aerodynamic performance of the compressor did not confirm the results obtained on the compressor rig tests. The reason for this was not discovered until it was decided to retest the actual engine test rig compressor on the compressor component rig. A contour discrepancy was discovered which was corrected by a remachining operation on the compressor vanes. This remachining operation was performed on the back-up stainless steel compressor because the titanium wheel was more sensitive to cracking problems. Both wheels were of the same design. The precise nature of the discrepancy, the aerodynamic effect, and a description of the rework operation are discussed in the Performance section of this report, paragraph 6.2.1.

As explained in paragraph 2.2.4, a key parameter in the life of the rotor thrust bearing is the control of axial load, which is the result of aerodynamic thrust on the rotor assembly. This load can be changed by adjusting the size of the scallops on the turbine wheel shown in Figure 6.

It was therefore decided that a measurement of the rotor thrust should be made before proceeding with more aerodynamic performance tests.

Rotor thrust measurement was obtained after instrumentation problems were resolved, as described separately in paragraph 4.6.

As the test program neared its conclusion, the engine test rig was prepared for a comprehensive test to evaluate the overall performance of the complete system.

This test was initially successful, but as the data were acquired a deterioration in performance was observed.

This deterioration was traced to the failure of a high temperature seal between the seal plate and the diffuser, and is discussed more fully in the Performance section of this report (Section 6).

Schedule and budgetary limitations prevented a further rebuild of the rig to obtain a final set of performance data, but each of the major components had successfully demonstrated the projected performances, and the test phase of the program was terminated.

Further details of the mechanical aspects of the program are presented in the Discussion section of this report (Section 5), and full information on the performance is contained in the section which deals specifically with that topic.

4.6 ROTOR THRUST MEASUREMENTS

During the early phase of the test program, the rig was modified to incorporate a strain gage, thrust-measuring device to evaluate rotor end thrust during rig operation. Figure 31 shows the strain-gage bearing retainer plate that was used to measure the axial load on the thrust bearing. The gages are in a two-gage bridge

Figure 31. Bearing Thrust Monitoring Device

to provide temperature compensation and are epoxy-cemented into position on three flexible tabs which support the bearing outer race. These tabs have a spring rate of approximately 750,000 lb/in. The tabs were spring-loaded to allow measurement of thrust loads in the range of ±50 to ±300 pounds. The thrust bearing is spring-loaded against a retainer plate by three belleville washers acting against a floating bushing between the bearing and housing.

During the initial mechanical check runs, bearing thrust load instrumentation was not working correctly and further problems were experienced with the epoxy adhesive, which was found to be unsuitable for this application.

The transducer gages were replaced and bonded with a high performance adhesive called M-bond 610, which is formulated specifically for bonding transducer strain gages in applications up to 450°F. Prior to assembly in the engine test rig, the strain gage circuits were checked in a laboratory oven for temperature compensation up to 300°F. Also incorporated into the current build of the engine test rig was an increase in the bearing thrust preload from 50 to 100 pounds. This allowed negative bearing thrust to be measured up to 100 pounds. On the third mechanical checkout run, the bearing thrust-measuring device, which was now operating satisfactorily, indicated a negative thrust (toward engine exhaust) of 30 to 35 pounds while the engine test rig was operating at approximately 70 percent speed. The rotor thrust measuring device indicated 64 pounds negative while operating at approximately 98.5 percent speed.

These loads are somewhat lighter than predicted but are at acceptable levels. It was also clear that the bearing load could be precisely controlled by turbine scallop modifications to meet the thrust matching requirements of an engine helical gear train.

5

DISCUSSION

Compared with the existing family of Titan engines, the advanced 60-kW engine test rig used several new design concepts selected because of anticipated problems which could result from the higher pressures and higher turbine rotor speeds.

The new designs included:

- The use of a Curvic coupling between the compressor and turbine.
- A different method of retaining the turbine nozzle.
- An encapsulated rotor bearing system.

The intent of these changes was to provide a rotor which could be balanced on its own bearings before assembly into the engine test rig and to ensure the balance integrity of the rotor throughout the speed range. Both of these concepts would ensure that bearing loads were within the required design limits, thereby providing long life. The new method of pinning the turbine nozzle was also considered to show benefits of ease of assembly, stability, and long life.

In retrospect it is clear that the development problems associated with these new ideas were seriously underestimated— to the point where at some stages the acquisition of aerodynamic performance data appeared to be in jeopardy. However, the mechanical problems were overcome and performance data were obtained.

A further review of the mechanical aspects of the rig operation is shown below.

5.1 ROTOR BALANCE

The use of Curvic couplings provides a rotor piloting device which offered significant advantages in that both axial and radial location is provided, combined with ease of disassembly/reassembly. Also, this type of coupling seemed to be less sensitive to potential balance changes resulting from the high rotor speed.

This capability was demonstrated on the initial balancing tests when the rotor was disassembled and reassembled without significant balance change. The tooth configuration and clamping load influence the curvic stability under stress, and, as mentioned previously, it was found to be necessary to increase the clamping load to maintain rotor stability under all operating conditions. This technique was satisfactory for rig operation but may not be the optimum solution. Gleason Works, the originator of the Curvic design, was consulted. Its recommendations were to apply the highest clamping load feasible without exceeding

the tooth contact stress limits of the material, to relieve the area surrounding the Curvic coupling for limited flexibility, and to change the profile of the tooth. The tooth profile change would be from an equally proportioned tooth (full barrel shape) to a biased design with increased retention on one side (3/4 barrel shape). This is consistent with the fact that the compressor (concave) is required to retain the turbine (convex), as the turbine has the greater expansion due to higher temperature at a similar modulus. A one-sided tooth (half barrel) was not recommended, partially because of possible transient conditions in which the compressor would be retained by the turbine.

The changes to the Curvic coupling design have been incorporated into the drawings in anticipation of future procurement of more development hardware.

In addition, a new turbine bolt has been designed which has the capability of exerting a higher clamping force on the assembled two halves of the coupling.

These changes are confidently expected to overcome any problems with rotor balance stability under all speed/temperature conditions.

5.2 TURBINE NOZZLE SHIFT

Migration of the static components, particularly the turbine nozzle, resulted from the new design method of nozzle piloting. A simplified approach was attempted which utilized six axial bolts through the diffuser and air inlet to provide radial location and axial retention. This approach was chosen in preference to the conventional method of radial pinning through the housing and diffuser because of the higher aerodynamic loading of the diffuser and higher operating temperatures on the nozzle, as well as the ease of aerodynamic clearance adjustment. The new method also eliminated the nozzle pin wear problem, which has been noted on high operating time engines over the years. However, the new design proved to be unsatisfactory and was rejected in favor of a return to a radial pin configuration for the duration of the tests. The standard radial pinning method may not be the best solution for a long life engine, but the design layout shown in Figure 32 is proposed as a further redesign which should be evaluated. This design allows free axial movement of the hot nozzle with respect to the diffuser and inlet while providing positive radial constraint without distorting the turbine shroud. This technique has been employed successfully on larger engines and should be directly applicable to this unit.

5.3 BEARING/SHAFT PROBLEMS

As discussed in paragraph 4.5, Rig Operational Tests, problems with rotor rubs were experienced and in some instances the turbine rotor bearing system failed.

Some failures may be attributed to the high radial loads caused by the balance shift problems resulting from inadequate clamping force on the Curvic coupling.

Other bearings were unsatisfactory because the hardness of the inner race was not within the drawing limits.

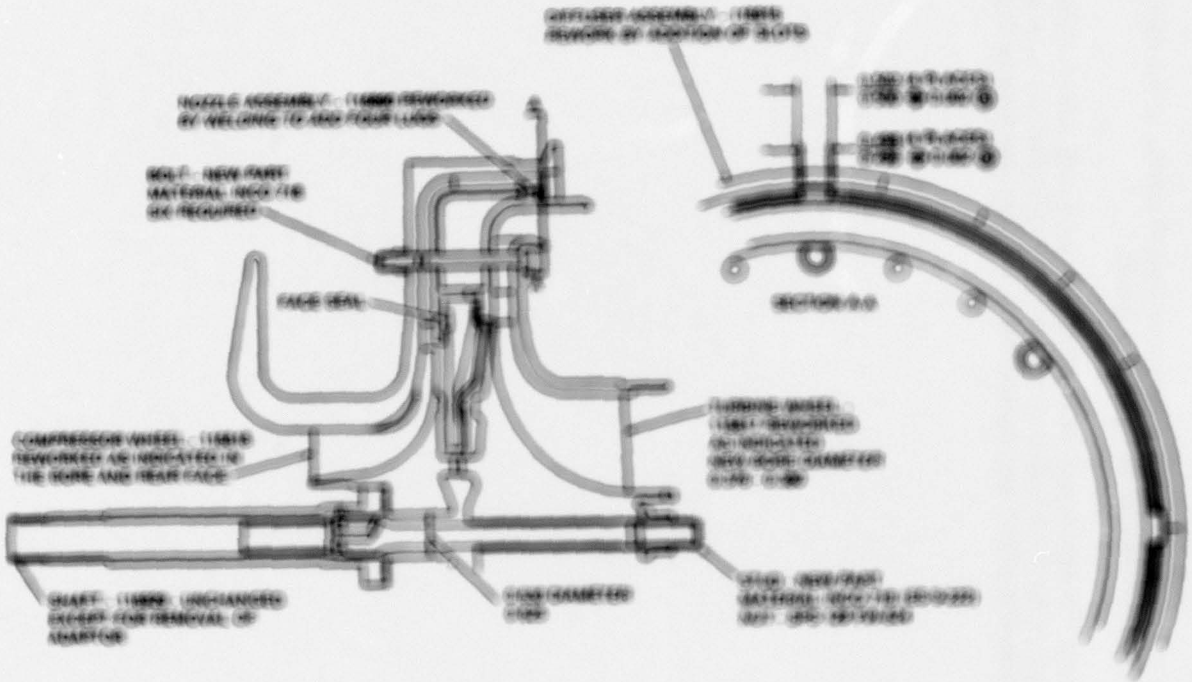

Figure 55. Proposed Design Changes for the Prototype Engine

The oil-dampened bearing support capsule was abandoned during the test since the cause of the rotor instability had not been isolated and an effort was made to eliminate new concepts which could have contributed to the difficulties.

However, other Solar high speed turbines, operating at speeds up to 80,000 rpm have used a similar oil-dampening system with a high degree of success. Further evaluation in Titan applications is warranted.

It has already been explained that thrust levels to be supported by the ball bearing can be controlled to an optimum level.

Although the problems encountered previously affected the progress of the over-all program, it is believed that these problems are now understood and will not significantly affect any future work on this new engine test rig.

6

PERFORMANCE

This section of the report presents a review of the predicted performance based on test rig data, the results of component tests from the engine test rig, and a table of projected engine performance for the new engine installed in a 60-kW generator set similar to the EMU/30-E.

6.1 ESTIMATED PERFORMANCE

Estimated engine performance was generated by matching the test rig compressor and turbine characteristics and using the following additional losses:

Burner pressure loss (%)	5
Burner efficiency (%)	97
Mechanical efficiency (%)	98

Estimated engine performance is shown in Figure 33 for corrected speeds of 105, 100, 95, and 70 percent design values. Output power at standard day conditions and 1080°F turbine inlet temperature is 100 horsepower with a corresponding fuel flow of 72 pph.

Estimated base engine performance at constant speed and varying air inlet temperature is shown in Figure 34 with lines of constant turbine inlet temperature and fuel flow. The estimated compressor surge limitation provides adequate surge margin under all anticipated engine operating environments.

Package installation losses equal to those of the T-62T-32 Titan engine installed in an EMU-30/E generator set were used to calculate overall generator set performance.

T-62T-32 installation losses at rated 60-kW output are:

Inlet pressure loss	3 inches of water
Exit pressure loss	6 inches of water
Compressor inlet heating	15°F

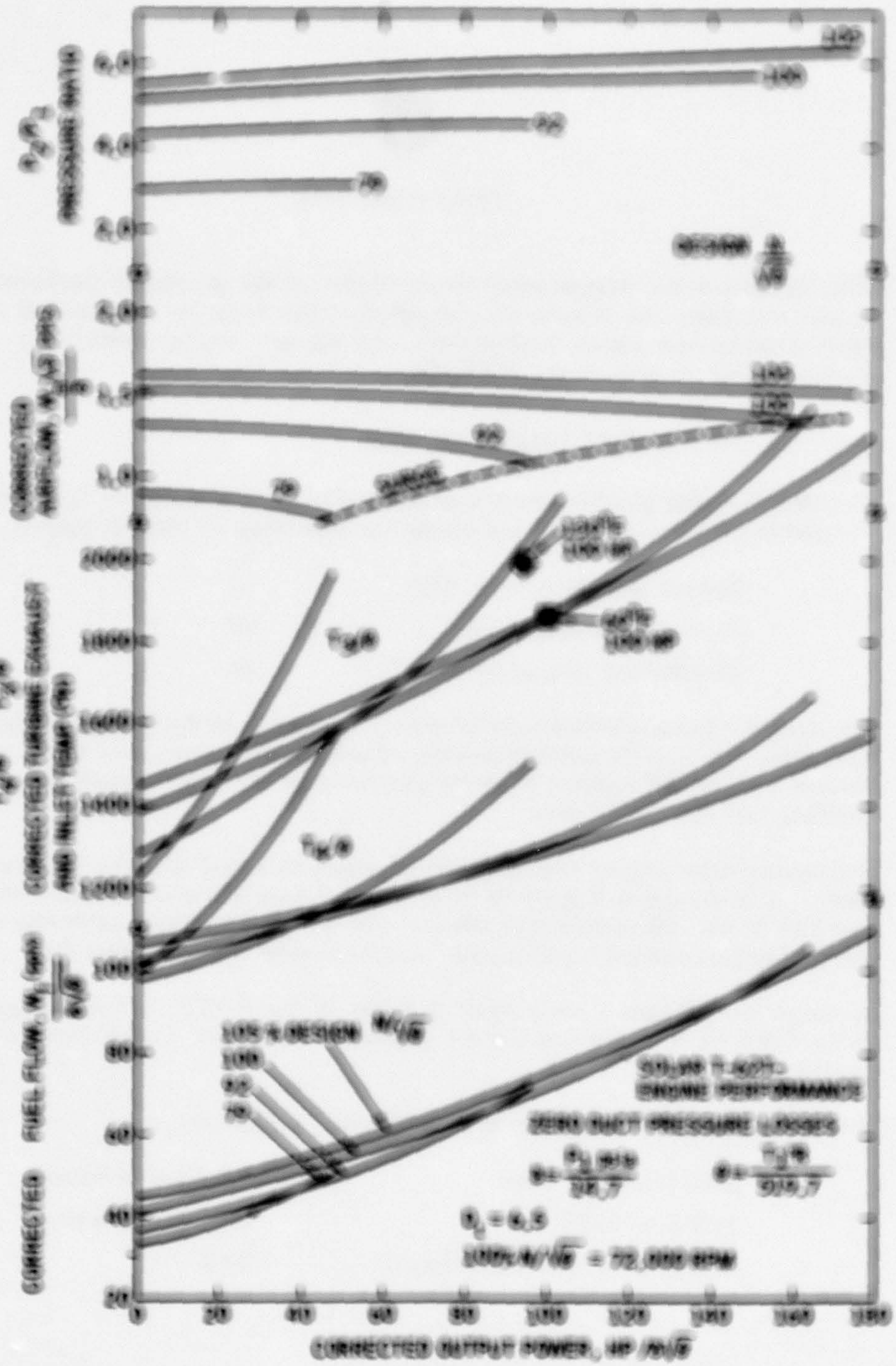

Figure 33. Engine Estimated Performance

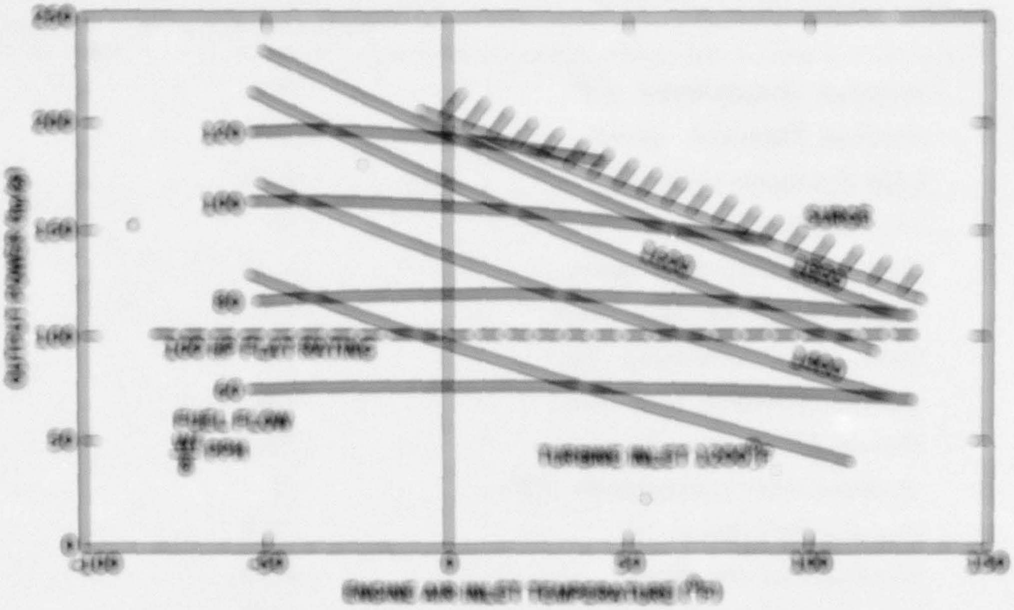

Figure 36. Effect of Inlet Temperature

Total equivalent power loss for these conditions is approximately 10 percent power at rated output. The estimated overall package performance with the above installation losses is listed in Table IV for both the sea level, 80°F and 5000 feet, 107°F conditions. Maximum turbine inlet temperature at the critical altitude day condition is 1960°F.

The capability of the uncooled, single-stage, radial-inflow turbine to operate at this maximum inlet temperature for the desired life is directly related to the tip speed, which, in turn, determines the turbine efficiency. The tip speed required to operate near peak efficiency at design point conditions is 2062 fps with a corresponding turbine velocity ratio, U/V_o, of 0.68.

6.2 TEST PERFORMANCE

The initial mechanical operating problems experienced on the engine test rig prevented performance calibrations at design speed and, in addition, both the compressor and turbine clearances were set high (0.020 and 0.055 inch respectively) to avoid rubbing. Nevertheless, some part-speed compressor performance data were acquired to check out the instrumentation and automatic data logging system. It was found that the system performed satisfactorily and that critical transducer pressure measurements agreed with backup manometer measurements.

Table IV.

Engine Cycle Conditions, Installed in EMU-30/E Generator Set

	SEA LEVEL/60°F	5000 FT/107°F
Ambient Temperature (°F)	60	107
Ambient Pressure (psia)	14.7	12.2
Inlet Pressure Loss (%)	0.75	0.75
Inlet Heating (°F)	15	15
Compressor Airflow (pps)	1.43	1.17
Compressor Pressure Ratio	5.4	4.8
Compressor Efficiency (%)	78	78
Burner Pressure Loss (%)	5	5
Burner Efficiency (%)	95.5	96
Turbine Inlet Temperature (°F)	1600	1940
Turbine Efficiency (%)	87.5	87.0
Turbine Velocity Ratio	0.69	0.656
Turbine Tip Speed (fps)	2042	2042
Turbine Exit Temperature (°F)	960	1212
Exhaust Pressure Loss (%)	1	1
Output Power (hp)	90.3	90.3
Output kW	60	60
Fuel Flow (pph)	72.0	71.4

The compressor, turbine, and overall engine performances of the major performance calibration builds are discussed as follows:

6.2.1 Compressor Performance. First performance data on the compressor (obtained 5-30-75) was a shroud clearance of 0.020 inch are shown on Figure 35 at 80, 90 and 100 percent design normalized tip speed. The overall performance was quite low - attaining a design speed pressure ratio and efficiency of only 4.45 and 70 percent. Analysis of the impeller and diffuser performances revealed that the diffuser static pressure recovery, C_{p2-E}, essentially equalled the baseline rig test data; thus, the large clearance of the impeller was suspected of materially reducing the impeller performance.

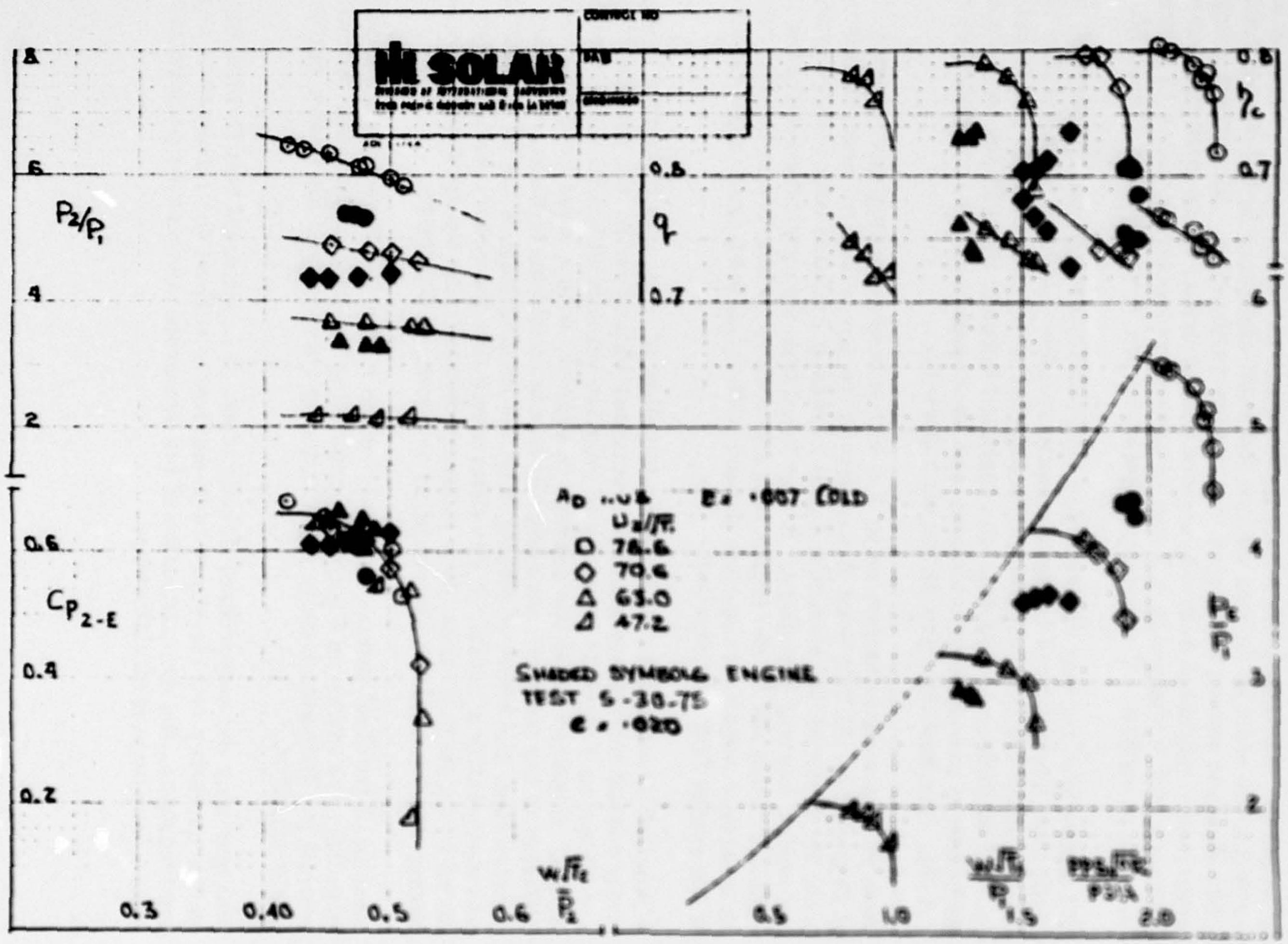

Figure 35. Compressor Performance (0.020-Inch Shroud Clearance)

Impeller axial clearance was therefore reduced to 0.014 inch on the next performance calibration on 6-3-75. The peak pressure ratio increased slightly to 4.6, see Figure 36. Examination of the compressor on subsequent stripdown revealed that the abradable shroud coating had not been touched; thus, it was decided to re-shim to further reduce the axial clearance to the design setting of 0.007 inch and return the engine test rig for calibration. Subsequent compressor performance (obtained 6-16-75) showed that at design speed peak pressure and efficiency had increased to 4.7 and 72 percent respectively with a 13 percent increase in airflow. The results of this test are also shown on Figure 36.

The engine test rig was returned for modifications to the turbine shroud, at which time inspection of the compressor revealed potential signs of flow recirculation from the discharge down through the seal plate O.D. to the impeller tip. An additional spring seal was installed between the diffuser backplate and seal plate to prevent recirculation, and the compressor was recalibrated on 4-8-76. The test data are shown on Figure 37.

Peak pressure ratio increased to 5.0 with a corresponding peak overall efficiency of 72 percent. At this point it was decided to reexamine all compressor components for dimensional accuracy and to carefully examine both compressor rig and engine test rig impellers. It was found that the original compressor rig impeller would not fit the engine test rig housing, which led to the discovery that an incorrect (smaller) impeller shroud radius had been used in the manufacture of the engine test rig impeller.

A detailed aerodynamic study of the impeller passage was instigated to quantitatively assess the influence of the discrepant shroud radii, the results of which are shown on Figure 38 in terms of relative velocity diffusion ratio versus shroud length. Constriction of the passage is evident, with a rapid reacceleration and diffusion at the point of maximum curvature (minimum radius). To delay the constriction, the effect of cutting back the leading edge of the 16 tip splitter blades was analytically studied. It was determined that the reacceleration could be reduced by 50 percent; thus, as a stop-gap measure the tip splitter blades of the backup steel impeller were modified as shown on Figure 39.

Results of the final compressor calibration (taken 10-27-76 with the modified impeller) are shown on Figure 40, indicating that the rig impeller diffuser and overall performance results were virtually repeated and the design performance goals satisfied.

Summarizing the compressor development, it is apparent that had the rig impeller geometry and clearance been duplicated without the influence of seal plate recirculation, the demonstration of the projected compressor performance level would have been straightforward.

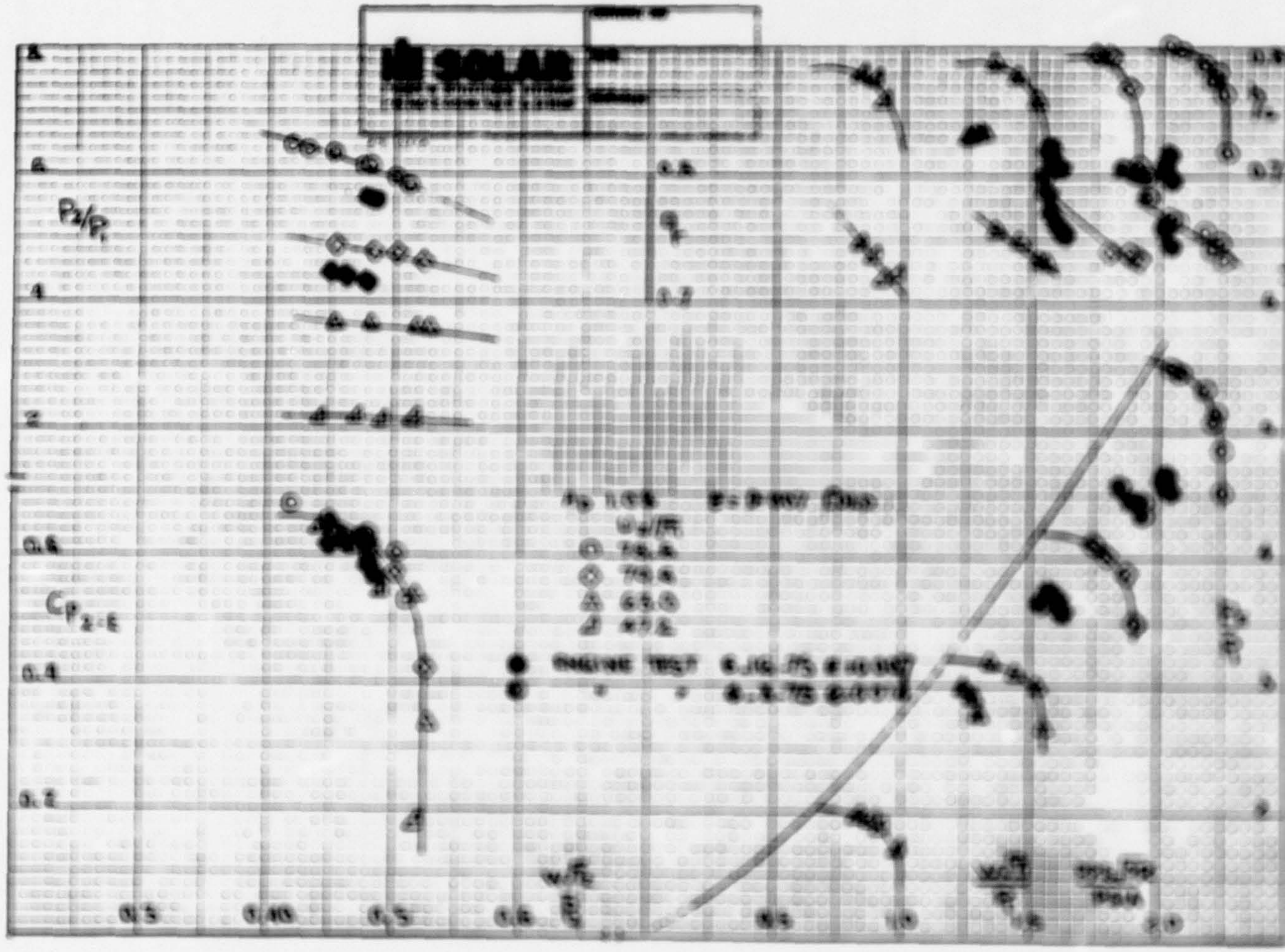

Figure 36. Compressor Performance (0.0[illegible]-Inch Shroud Clearance)

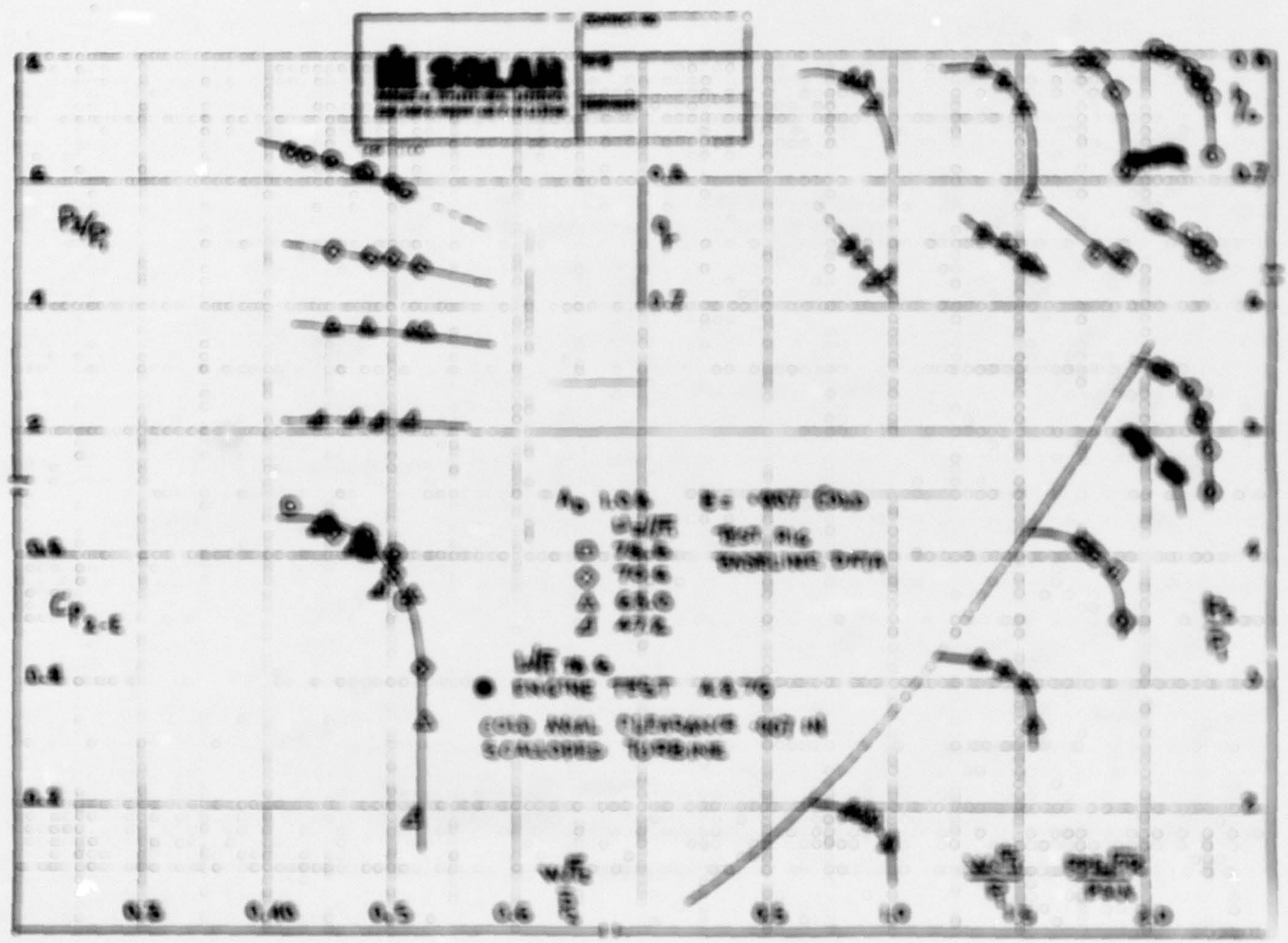

Figure 37. Compressor Performance (With Additional Spring Seal)

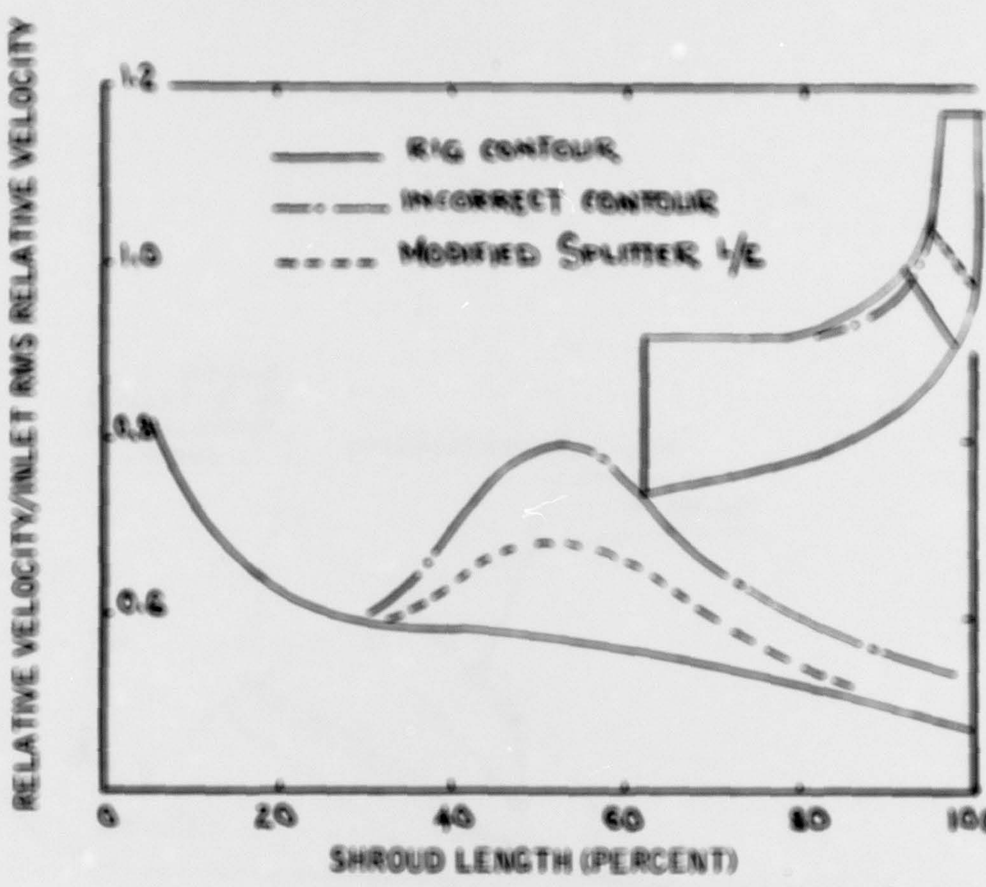

Figure 39. Effect of Shroud Curvature

6.2.2 Turbine Performance. First turbine component performance calibrations were conducted on 6-2-75 with the unscalloped shroud configuration. Test performance data from the engine test rig (shaded symbols) are compared with the baseline rig data on Figure 41. Peak overall turbine total-static efficiency was 88.5 percent, exceeding the design goal of 87.5 percent. Turbine inlet flow function matched that required for optimum engine matching. A second turbine calibration was made on 3-3-76, the results of which are shown on Figure 42 showing a slightly lower peak efficiency of 87.5 percent.

Following the test program plan the turbine disc was subsequently scalloped to the design dimension of 5.4 inches, but for reassembly the seal plate heat shield was not installed, leaving a large effective clearance between the turbine disc and seal plate. The results of the scalloped turbine configuration performance calibration of 4-8-76 are shown on Figure 43, indicating that the peak overall turbine efficiency dropped to 85.2 percent with no significant change in the inlet flow function.

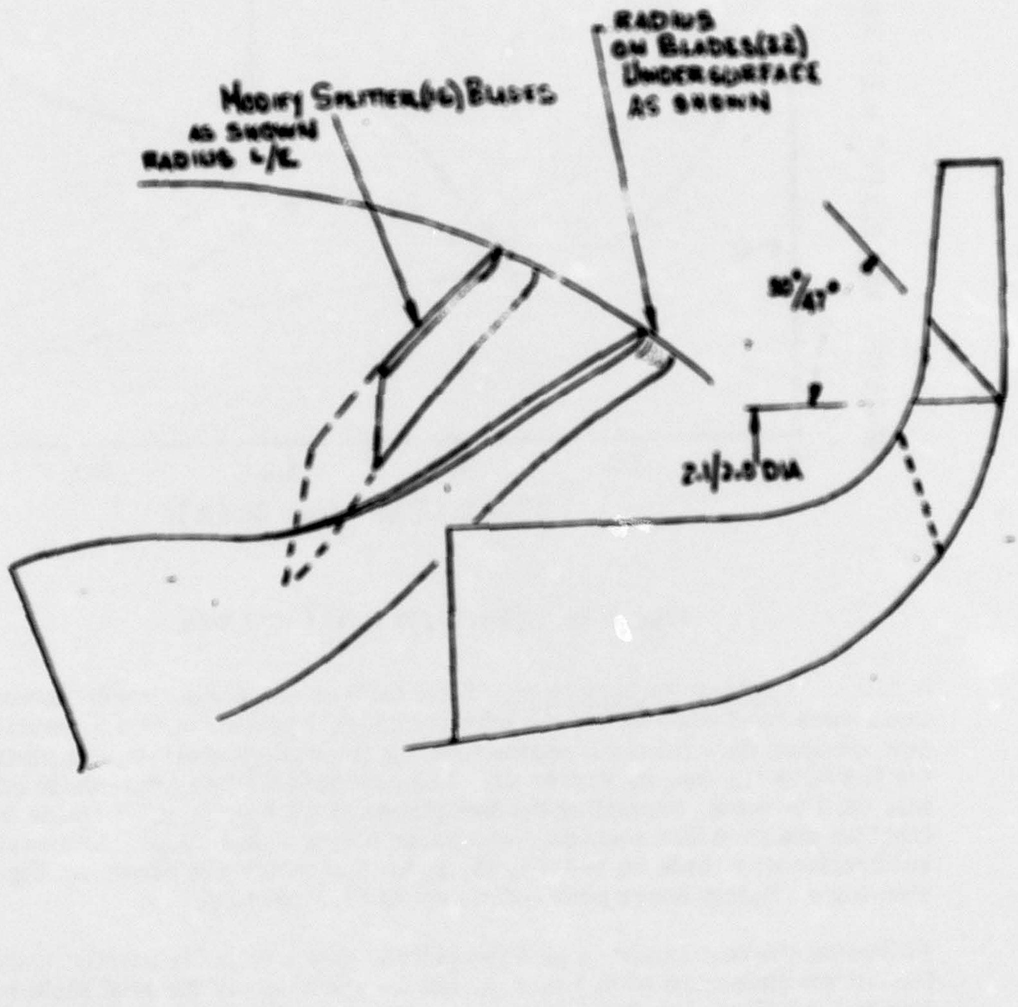

Figure 39. Impeller Modification

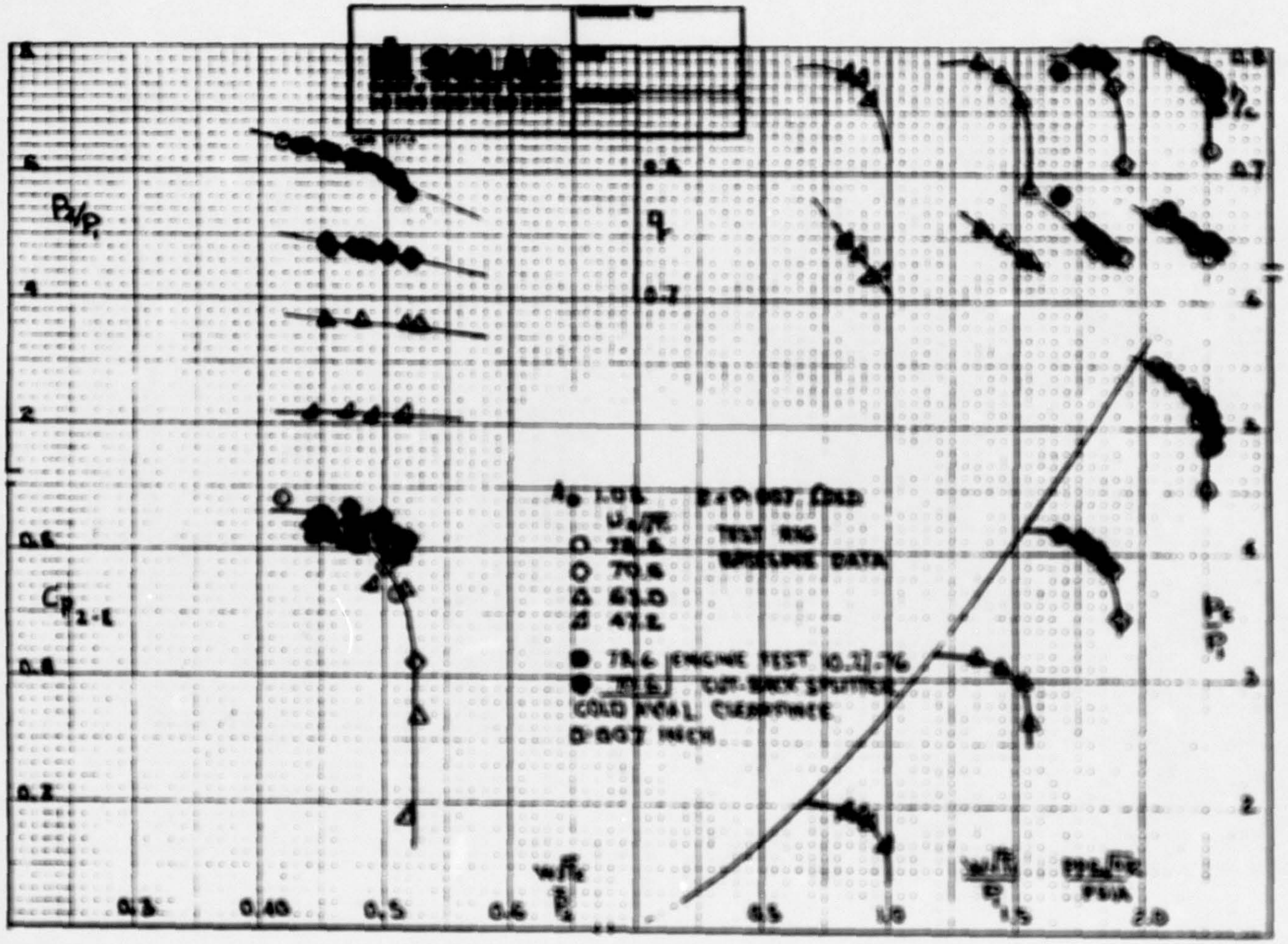

Figure 40. Final Compressor Calibration

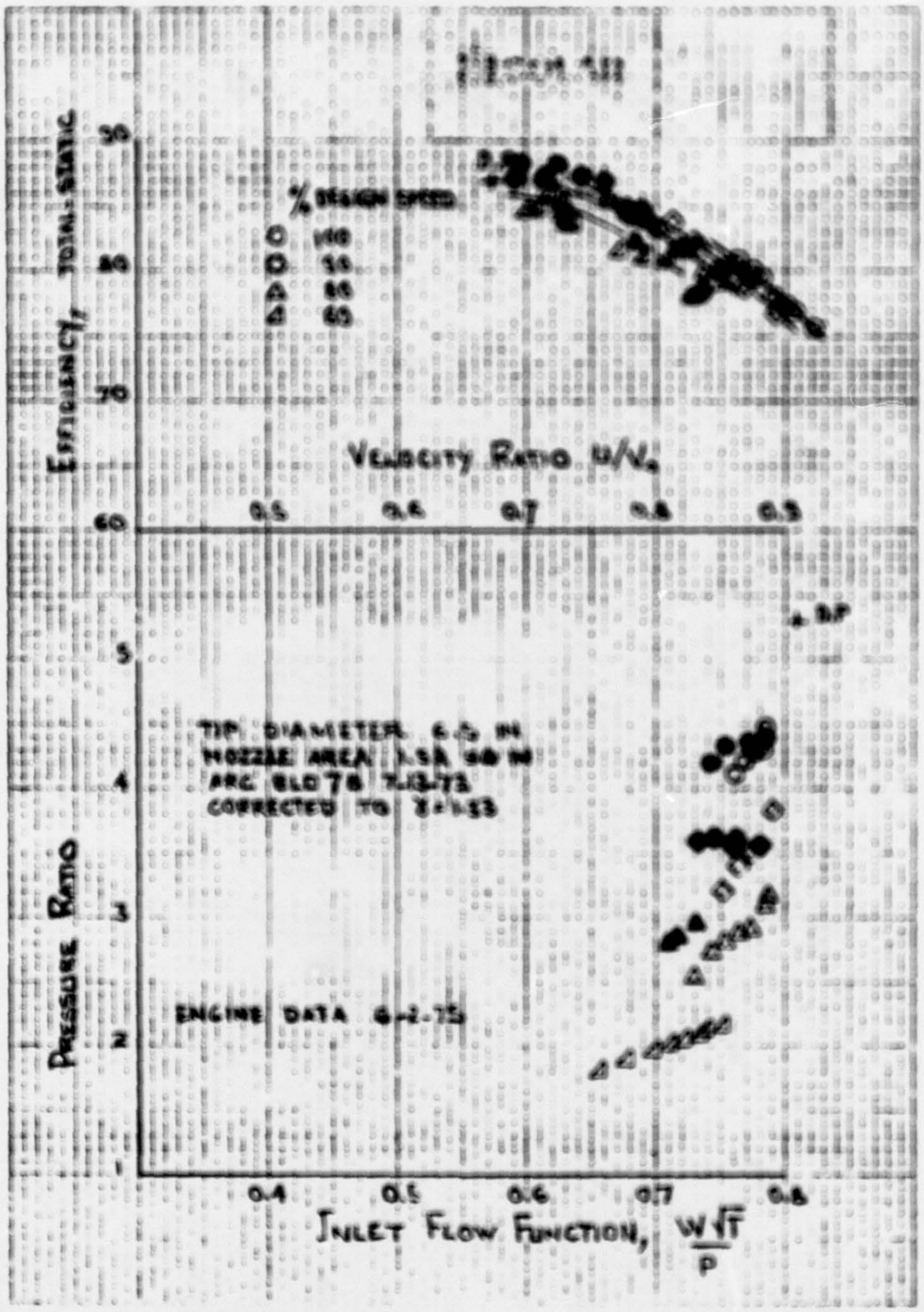

Figure 41. Turbine Performance (First Calibration)

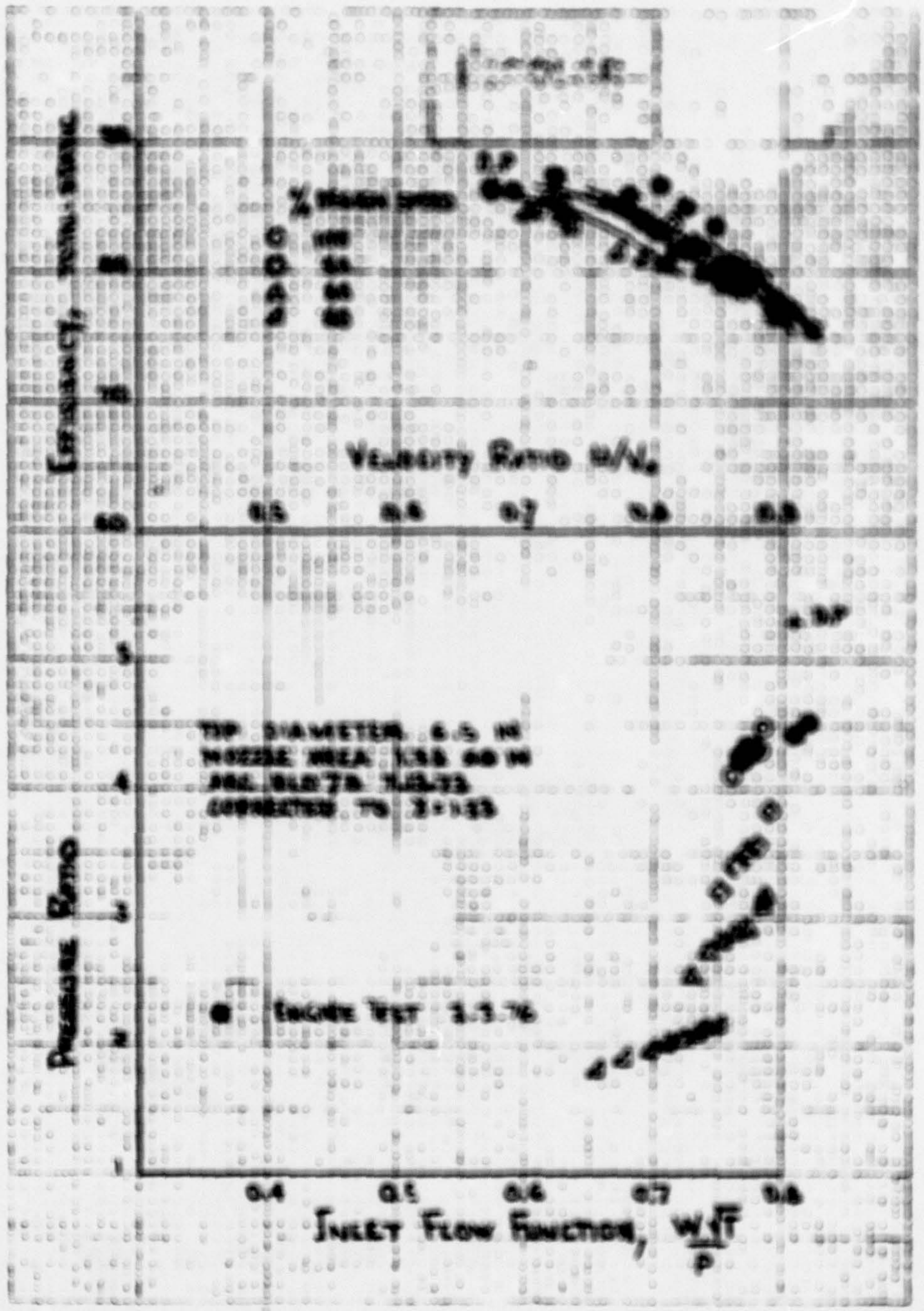

Figure 42. Turbine Performance (Second Calibration)

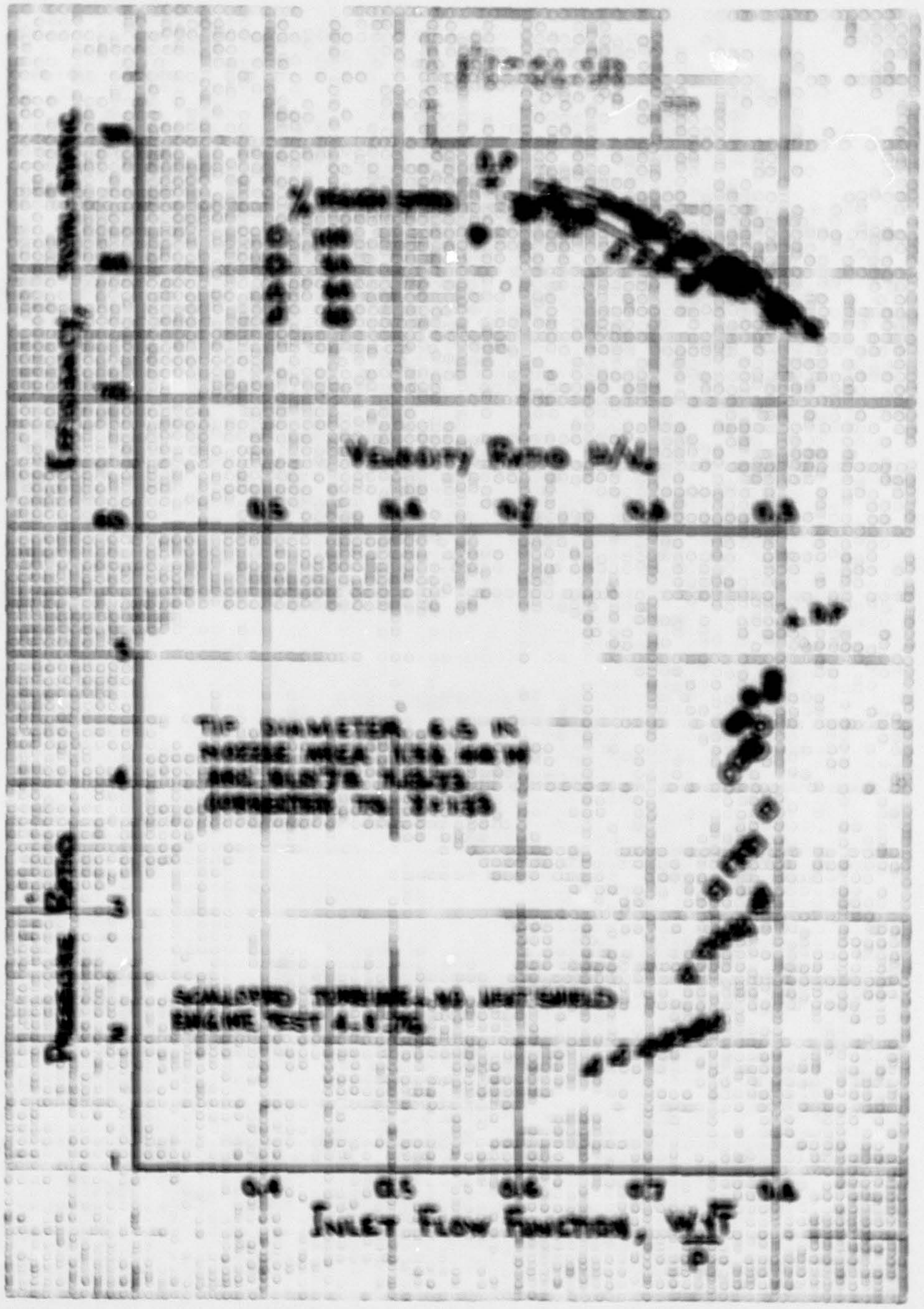

Figure 43. Turbine Performance (Scalloped Configuration)

The final test of the engine test rig to evaluate the compressor and turbine together was a minor disappointment when, on 10-27-76, design compressor performance was achieved. But it was apparent that on loading the engine past approximately 60 hp, an internal turbine leak was occurring, adversely affecting the turbine performance which had hitherto fulfilled design expectations. Overall turbine efficiency is shown on Figure 43, indicating a peak level of 86 percent prior to occurrence of the internal leak. The leak was traced to failure of the commercial high temperature seal between the seal plate and diffuser. Several unsuccessful attempts were made to seal this in place, and eventually a teardown inspection of the unit revealed that the nozzle regrinding operation on the most recent build had been improperly carried out, resulting in an irregular gap around the seal plate. This resulted in an overload on one side of the seal and a very light load on the other, causing failure.

Because of the seal failure, engine performance data were not obtained with both compressor and turbine components operating together, but the data from the individual components met design specifications separately, and the final engine performance projections are based on these data.

6.2.3 Engine Performance. The results of the major engine performance calibrations are shown on Figures 44, 45, and 46. The best specific fuel consumption attained was 0.77 lb/hp-hr at 100 hp, sea level, 60°F uninstalled conditions, compared with the Solar design goal of 0.71 lb/hp-hr.

Test data from the final calibration, with the internal leak occurring above approximately 60 hp, are shown on Figure 44 compared with the design prediction. It is apparent that the design engine performance predictions were equalled below the leak point and, had the leak not occurred, the full load engine performance would have been demonstrated.

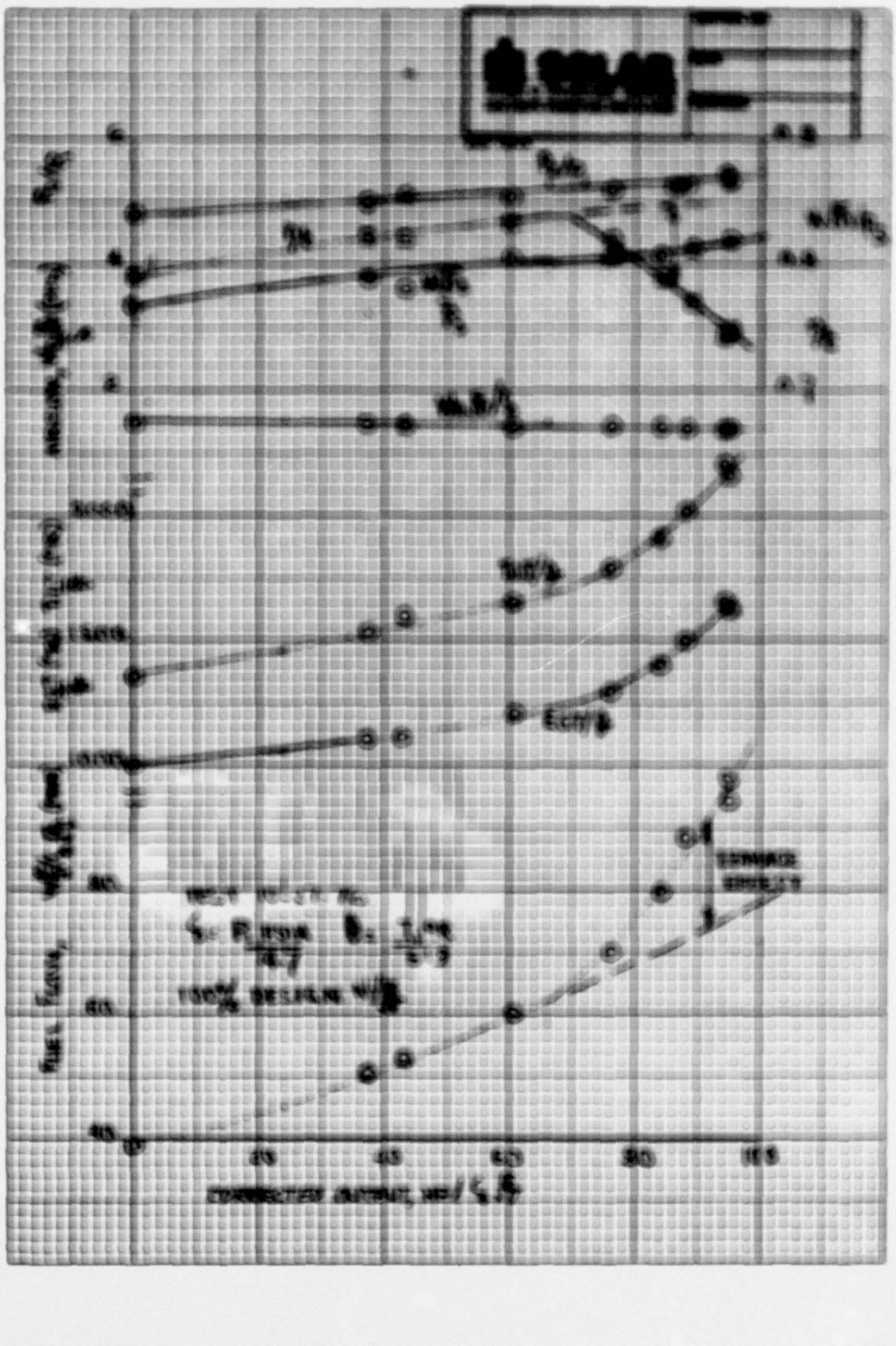

Figure 44. Engine Performance (Final Calibration)

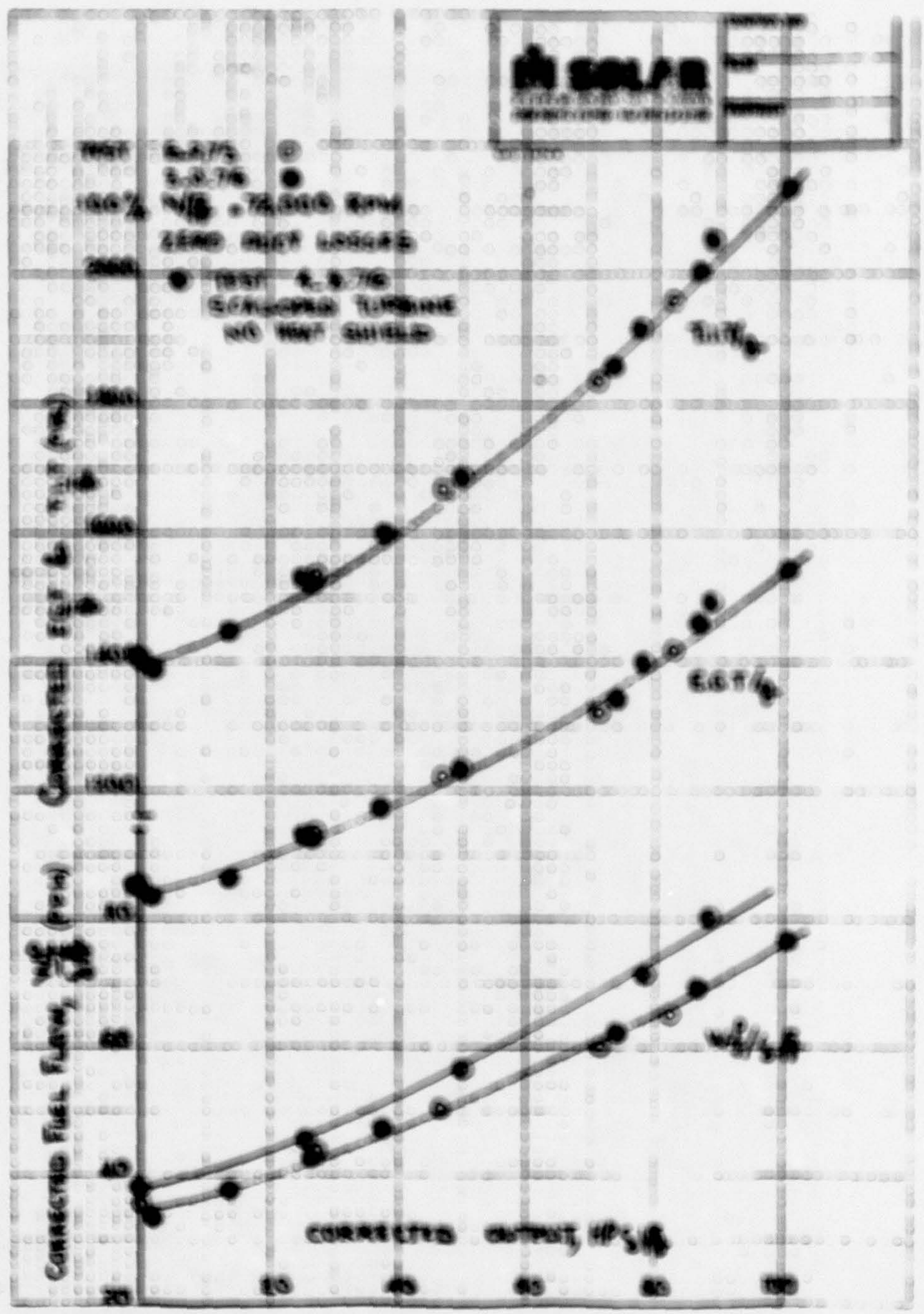

Figure 45. Engine Performance Test Data

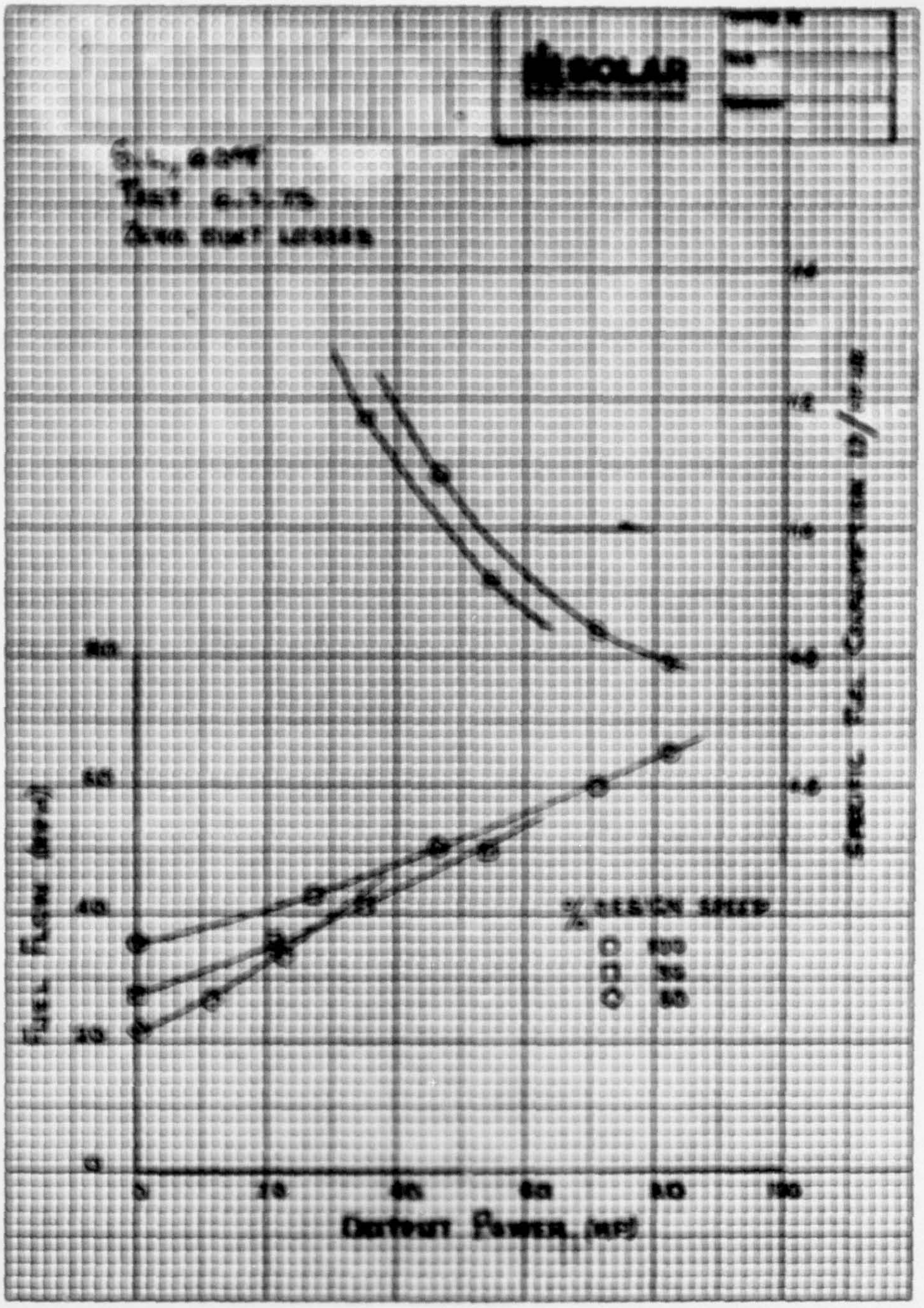

Figure 46. Advanced Turbine Test Performance Data

7

PRELIMINARY ENGINE DESIGN AND PACKAGING

This compressor development program was initiated to create the primary component for an advanced 60-kW gas turbine engine with reliability and low fuel consumption. As a part of the contract a preliminary design for an engine utilizing this component was to be established. The advanced 60-kW engine test rig on which testing was performed represents not only a preliminary design but prototype hardware for the turbine section.

A layout of the proposed engine is shown in Figure 47. The turbine section of this layout is essentially the engine test rig component as tested. The combustor is an undeveloped unit but is basically the same design employed on the existing T-62T-32 engine used in the EMU-30/E generator set. Modifications will be required to the combustor to enable it to operate at the higher turbine inlet temperature and case pressures. The reduction drive assembly is also the existing T-62T-32 unit with a new primary reduction stage. Double-reduction gearing is necessary to reduce the 72,000 rpm rotor speed to the 6000 rpm requirement of standard generators.

The basic cycle analysis for the proposed advanced 60-kW engine has already been discussed, and the performance shown in Table IV confirms that the objectives for both standard day and worst conditions can be met.

Packaging of the advanced 60-kW engine is straightforward. The advanced engine is a direct replacement for the existing T-62T-32 in the EMU-30/generator set. It will be necessary to change only the primary reduction gearing and power section, the fuel control, and the interconnecting fuel and air lines. The additional length of the primary reduction gear is compensated for by the shorter combustor.

The advanced engine represents a direct retrofit for existing units and the least expensive approach to a new generator set because new packaging design is not required.

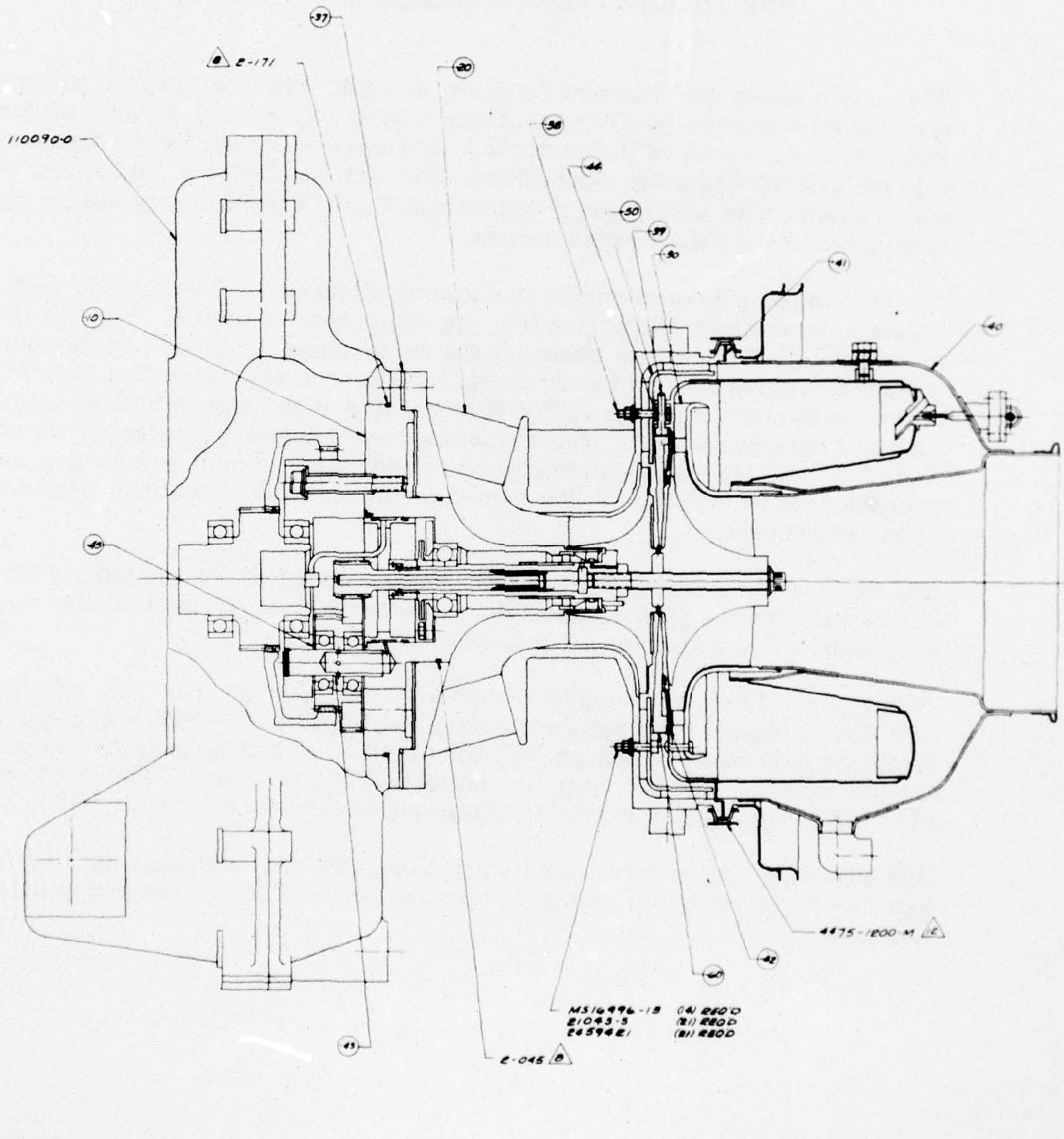

Figure 47. Advanced 60-kW Engine Cross Section (Sheet 1 of 2)

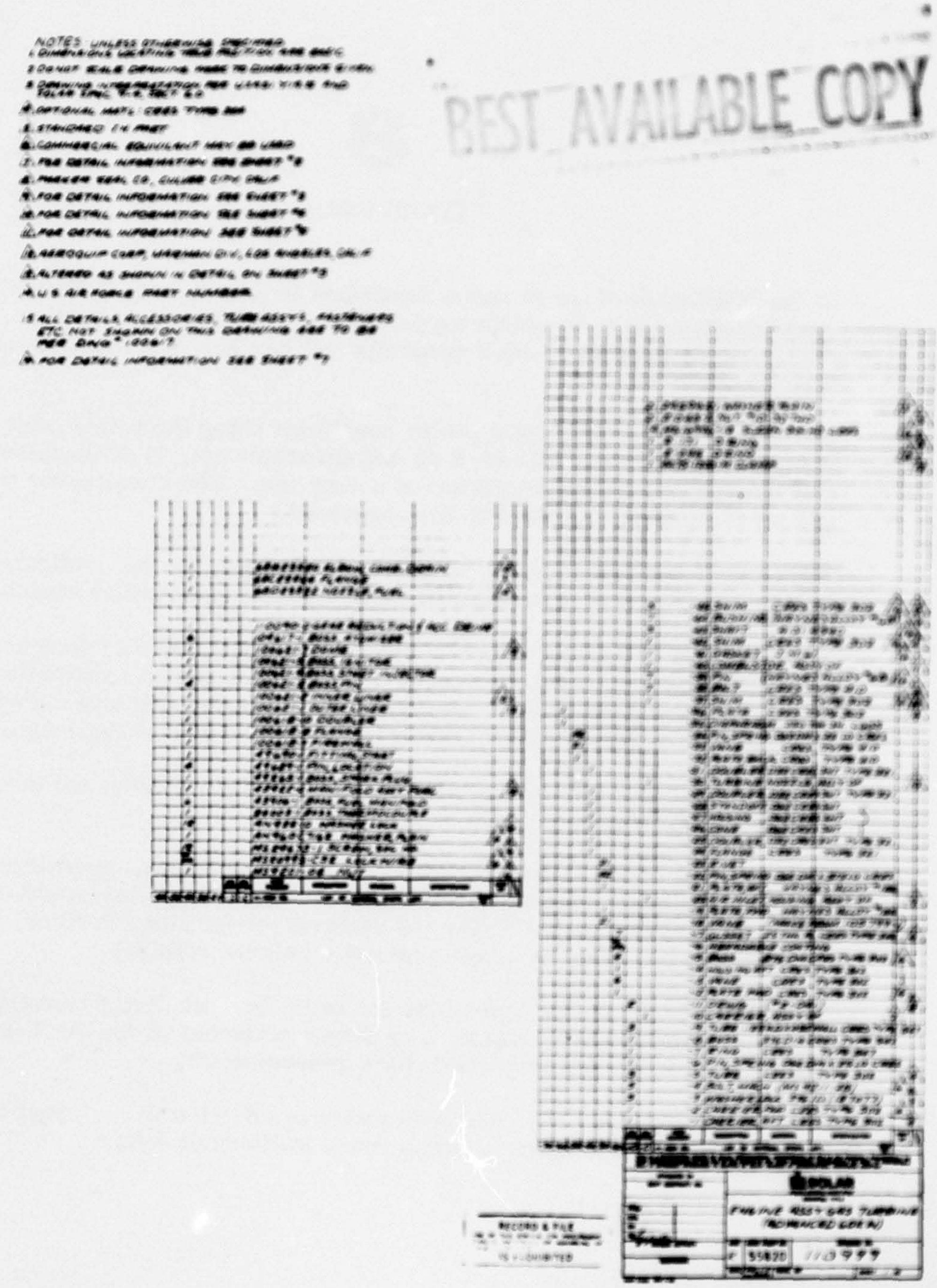

Figure 47. Advanced 60-kW Engine Cross-Section (Sheet 2 of 2)

8

CONCLUSION

At the conclusion of the program described in this report, sufficient test data had been accumulated to demonstrate that the new compressor, turbine, and complete engine for an advanced 60-kW generator set had successfully achieved the performance objectives.

Fuel flow at sea level, rated power conditions using the actual inlet and exhaust pressure loss of the EMU-30/E 60-kW generator set, is projected at 72 pph, which was the goal set by the procurement documents. The compressor pressure ratio is 5.4, compared with the 5 to 6:1 suggested.

The overall performance provided by this advanced engine configuration promises to be a significant step forward in small military gas turbine engine technology.

The progress of the test program cannot, however, be described as trouble-free. The difficulties encountered were generally the result of an attempt to implement too many mechanical design improvements into an engine test rig where even the basic performance objective presented a major technical challenge.

These mechanical difficulties were systematically resolved and the operation of the engine test rig was finally successful.

In addition to the successful performance demonstration, several innovative engineering improvements were implemented, the most important of these being the use of a Curvic coupling for the compressor-turbine interface, which offers an excellent potential for long-term rotor balance stability.

The engine test rig now represents the basis for a realistic prototype engine which can, with further development, be a direct replacement for the T-62T-32 Titan engine used in the military EMU-30/E generator set.

Such a replacement effort has been shown to offer the Government the prospect of long-term cost savings involving many millions of dollars.